TOOLS FOR THE IMPROVEMENT OF FLAVOR IN INTERSPECIFIC HYBRID GRAPE VARIETIES: A *POST HOC* ANALYSIS METHOD FOR QUANTITATION OF VOLATILES AND A PROFILE OF MALATE DURING BERRY MATURATION ACROSS *VITIS* SPP.

A Dissertation

Presented to the Faculty of the Graduate School

of Cornell University

In Partial Fulfillment of the Requirements for the Degree of

Doctor of Philosophy

by

Elizabeth Ann Burzynski Chang

August 2019

TOOLS FOR THE IMPROVEMENT OF FLAVOR IN INTERSPECIFIC HYBRID GRAPE VARIETIES: A *POST HOC* ANALYSIS METHOD FOR QUANTITATION OF VOLATILES AND A PROFILE OF MALATE DURING BERRY MATURATION ACROSS *VITIS* SPP.

Elizabeth Ann Burzynski Chang, Ph.D.

Cornell University 2019

Interspecific hybrid grape varieties (*Vitis* spp.) are cultivated by grape breeding initiatives due to wild *Vitis'* resistance to abiotic and biotic stress. However, these cultivars suffer from multiple flavor challenges, such as off-aromas and excessive sourness in the final wine product. When profiling volatiles in hybrid mapping populations, we performed headspace solid-phase microextraction (HS-SPME) coupled to gas chromatography–mass spectrometry (GC-MS), and quantitated select off-odorants using matched, isotopically labeled isotopologues. Seeking to move toward a less targeted approach, we tested the assumption that any relative changes in matrix effects among individuals would be similar for all compounds, i.e., matrix effects do not show Compound × Individual interactions. Individuals from two plant populations were analyzed: an interspecific grape (*Vitis* spp.) mapping population (n = 140) and a tomato (*Solanum* spp.) recombinant inbred line (RIL) population (n = 148). Individual plants from the two populations were spiked with a cocktail of internal standards (n = 6, 9, respectively) prior to HS-SPME-GC-MS. Variation in the relative responses of internal standards indicated that Compound × Individual interactions exist, but were different between the two populations. For the grape population, relative responses among pairs of internal standards varied considerably among individuals, with a maximum of 249% relative standard deviation (RSD) for the pair

of [U^{13}C]hexanal and [U^{13}C]hexanol. However, in the tomato population, relative responses of internal standard pairs varied much less, with pairwise RSDs ranging from 8% to 56%. This *post-hoc* methodology can be applied to evaluate the suitability of using surrogate standards for HS-SPME-GC-MS studies in other plant populations.

A related project evaluated the development of malate in wild *Vitis* spp. during berry maturation. Over a two-year study, samples from *V. riparia*, *V. cinerea, V. vinifera,* and hybrid spp. were taken at multiple time points. In contrast to the well-known biphasic behavior of malate in *vinifera*, we observed a range of behaviors in wild species. On average, *riparia* accessions had malate per berry comparable to *vinifera* just prior to veraison, but degraded malate at a slower rate. *Cinerea* accessions had significantly lower malate prior to veraison than all other groups, but showed a post-veraison increase in malate. Post-veraison malate degradation rates of interspecific hybrids were intermediate to *vinifera* and *riparia*. Variation in post-veraison malate behavior could be related to diminished malate degradation in the pulp of wild *Vitis spp*. Our results indicate that studies of malate behavior in *Vitis* spp. and their hybrids should include both pre- and post-veraison time points.

BIOGRAPHICAL SKETCH

Beth [Burzynski] Chang joined the lab of Dr. Gavin Sacks in the Department of Food Science at Cornell University in 2014. She studies grape and wine flavor chemistry, primarily focusing on off-aromas and sourness in *Vitis* spp., with an additional project developing food safe labs for high school chemistry classes. Beyond academics, Beth has been heavily involved in GPWomeN: the Graduate and Professional Women's Network at Cornell University. She served on the executive board for three years, and secured a leadership grant for a collaborative speaker series during her tenure as President of the organization. Beth is a recipient of the American Wine Society Educational Foundation scholarship, the American Society for Enology and Viticulture's Best Student Oral Presentation in Viticulture award, as well as an International Women's Day Leadership award. Prior to her Ph.D., Beth earned a B.A. in Psychology from Cornell University, a M.S. in Chemistry from Villanova University, and a Level 3 certification from the Wine and Spirit Education Trust, and worked in hospitality management. Upon completion of her degree, Beth will be assuming the position of Enology Extension Specialist in the Department of Food Science at Virginia Tech.

To my LECO Pegasus, Peggy, and my beloved dog, Bertie.

The former honed my grit and perseverance, and in doing so, fostered self-confidence; the latter was there for me in the darkest hours and brightest days alike – an unconditionally loving furball who gives me balance, perspective, and so much joy.

ACKNOWLEGEMENTS

I am so thankful for my advisor, Dr. Gavin L. Sacks. Thank you for allowing me to join your lab, and for your never-ending patience, amazing dry humor, critiques of my work, nurturing of my career ambitions, and occasional ’90s references.

I also thank my minor committee members, Dr. Robert A. Raguso, and Dr. J. Thomas Brenna. I greatly enjoyed taking both of your classes, and I appreciate your valuable perspectives on my research aims, as well as your support of my long-term goals. Also, I acknowledge Dr. Robin Dando, my field appointed committee member, who provided good recommendations regarding the logistical feasibility of my work.

I thank Dr. Justine Vanden Heuvel, who has been a great mentor, giving me candid advice and enthusiastic support throughout my time in the program. Similarly, I am grateful to Aaron Jacobsen, Erin Atkins, and Dwayne Bershaw for always welcoming my random questions and requests with a friendly smile and helping hand. Also, many thanks to Dr. Anna Katharine Mansfield for her wholehearted support and honest counsel during this last year; I look forward to picking her brain for years to come.

I am eternally grateful to my $S_n$acks lab family. I always say that you – all of you – make the bad days good, and the good days better. Thanks for the mentorship, the friendship, the Wine Fridays, and the ceaseless treats and laughter.

I extend my deepest gratitude to my family: my parents, Charlie and Kathy, and my sisters, Elyse and Caitlin. You have been firmly on Team Beth Ann since Day 1 of my graduate school experience, and that strength of conviction and reassurance has been a guiding force throughout the ups and downs of the past 7 years. I also acknowledge my Aunt Jani, who provided encouragement and excellent advice at key points throughout the journey. And most of all, I give my love and thanks to my husband, Chris. You are my rock; your unwavering support of this Ph.D., and the sacrifices that you have made to help it happen, are everything to me.

TABLE OF CONTENTS

LIST OF FIGURES

LIST OF TABLES

CHAPTER 1

INTRODUCTION

Breeding for flavor: screening of interspecific hybrid grape mapping populations

Mapping populations are used by plant breeders to improve fruits and vegetables such as apples [1,2], tomatoes [3], grapes [4], melons [5], peaches [6], and peppers [7]. These mapping populations frequently contain hundreds of individuals (i.e. accessions), where each individual has a unique genetic composition from the crossing of a set of parents. Genomics-assisted breeding tools [8], such as genome wide association studies (GWAS) [9,10], or marker assisted selection (MAS) [11,12] are used to select for traits of interest, such as size, firmness, postharvest shelf life, and more recently, flavor [13,14]. The phenotypic data is screened against molecular markers on the chromosomes that correlate with variance in the trait, called quantitative trait loci (QTLs). In some cases, a single QTL may drive trait expression, such as monoterpene content in grape berries [4,15]. More frequently, multiple QTLs are found to control a phenotype, such as mealiness in peaches [6].

One such breeding initiative has been the development of interspecific hybrid grape varieties, which are a cross between the well-known European *Vitis vinifera* species with wild *Vitis* species that have grown indigenous to North America for thousands of years. These wild *Vitis* species have adapted to the North American climate, and often have traits of interest such as cold hardiness, and resistance to diseases endemic to our climate, such as phylloxera, downy mildew, black rot, and powdery mildew [16]. However, there are several major organoleptic challenges associated with wild *Vitis*, which may also appear in their interspecific hybrid grape

offspring. Red wines made from hybrid grape varieties are reported to have poor mouthfeel, which results from low tannin concentrations in their fruit and higher concentrations of tannin-binding pathogenesis-related proteins [17,18]. Wines made from hybrids with *V. labrusca* parentage suffer from excessive grape and "foxy" off-aromas [19] due to high concentrations of methyl anthranilate and 2-aminoacetophenone. Hybrids containing non-*labrusca* wild *Vitis* spp., e.g. *riparia*, *rupestris*, and *cinerea* tend to have high concentrations of methoxypyrazines, which cause the final wine product to smell green and herbaceous [20]. Finally, it has been reported since the late-1960s that many wild *Vitis* spp. have 3-4 times the titratable acidity (TA) of their domesticated *vinifera* counterpart, and that this higher TA is mainly attributed to higher concentrations of malate in the ripe grape berry [21,22]. This high TA correlates to a perception of excessive sourness in the final wine product that is difficult to ameliorate through TTB-approved winemaking practices [23,24].

Prior work in our lab has proposed remediation strategies for better tannin extractability to improve mouthfeel in interspecific hybrids [25]. Likewise, we had previously devised a screening for key off-odorants in mapping populations that were used by collaborators to identify several putative QTLs related to a lipid degradation pathway that result in high concentrations of the volatiles responsible for green and grassy aromas in the ripe grape berry (S. Yang, personal communication, 12/17/15). This screening used headspace solid phase microextraction (HS-SPME), a frequently employed technique due to its simple and solvent free extraction process, feasibility of automation, and the small amount of sample material needed [26,27]. When coupled

to gas chromatography-mass spectrometry (GC-MS), a single sample run can provide a profile of the volatiles present in plant material [1,28].

However, SPME is known to suffer from matrix effects, especially in complex plant matrices [27,29–31], and therefore internal standards are recommended for quantitation. In our prior work, we quantitated eight compounds in each mapping population using isotopically labeled isotopologues. This is considered a best practice, however these standards are expensive, difficult to procure, and/or need to be synthesized [26,32]. In the case of evaluation of multiple mapping populations for a plant species, this method rapidly becomes impractical because it limits the scope of work to a small, target screen, and limits the ability to pursue novel analytes that may also be influencing fruit quality.

Due to these challenges, breeders often utilize alternative strategies for quantification, such as quantitation against a single (often unlabeled) internal standard [10,33], by comparison to an admixture reference sample [3], or else normalize analyte responses to the total ion count [5,30]. When using a single surrogate standard, it has been assumed that although SPME-induced matrix effects may affect the relative response of compounds from individual to individual (i.e. from run to run), all compounds will be equally impacted (Figure 1). However, to our knowledge, this assumption had not yet been tested, and therefore formed the premise of Chapter 2.

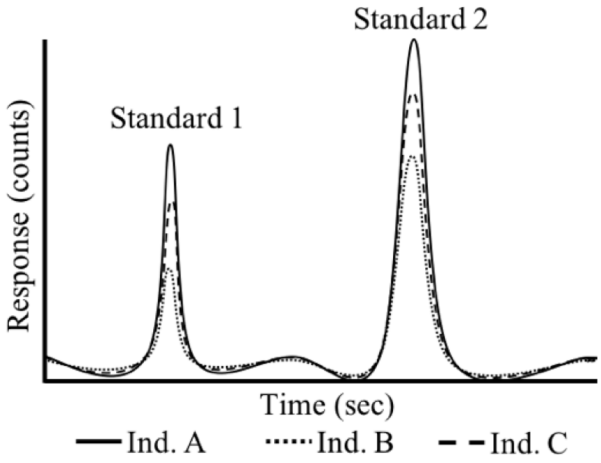

Figure 1.1: Assumption of equal across-individual matrix effects using HS-SPME.

Elucidating the evolution of malate across berry maturation in wild Vitis spp.

As previously mentioned, a third flavor challenge of interspecific hybrid grapes is the high level of titratable acidity (TA), and resulting perception of excessive sourness on the palate. In wild *Vitis* species, it has been reported that TA can approach 50 g/L, as tartaric acid equivalents, even at total soluble solids (TSS) levels that are associated with fully mature fruit (TSS > 20 Brix) [20]. This is considerably higher than the TA range of 6-9 g/L typically observed in mature *V. vinifera* [21]. The major organic acids in the grape berry are tartrate, malate, and citrate, and of these, the acid with the highest concentrations and most variation is malate, and the organic acid that varies most, is malate [21,22]. In wild *Vitis*, malate can be present at concentrations > 20 g/L in mature fruit [22], and similarly, interspecific hybrids are reported to have higher malate than their *V. vinifera* counterparts at harvest (5.0 – 7.3 g/L vs. 2.7 – 4.2 g/L), even when grown on the same site with similar cultural practices [34].

In winemaking, high malate in grapes is of greater concern than high concentrations of the other major grape acid (tartaric), as the latter generally has a limited concentration range in wines due to the low solubility of potassium bitartrate in hydroalcoholic solutions [35]. Remediation strategies for high malate, such as malolactic fermentation and 'double-salt' precipitation, are not appropriate for all wines and can still result in high TA even once complete [36]. Thus, producing hybrid grapes with lower malate is of interest to the wine industry, either through use of appropriate viticultural practices or through breeding of new grape varieties.

In *vinifera*, malate exhibits a biphasic pattern, with initial accumulation in the vacuoles of immature fruit, primarily in the mesocarp [37]. Starting at veraison, malate concentrations decrease largely because berries switch from accumulating to degrading malate, and also because of dilution due to berry expansion [38]. However, a molecular explanation for the high malate of mature wild *Vitis* spp. and their hybrids has not been presented. Quantitative trait loci (QTL) analyses of *Vitis* spp. populations have been ambiguous – one study of a Seyval F2 mapping population identified a weak QTL in a region containing a gene associated with an aluminum-activated malate transporter (ALMT) [39]; another identified several minor QTLs for malate, but were unable to assign these to specific candidate genes [40]. One limitation of these studies, and related existing work, is that only post-veraison, mature fruit was sampled, and therefore the typical behavior in malate during berry maturation in *Vitis* species other than *vinifera* has not been characterized. Therefore, in Chapter 3, we sought to characterize the developmental profile of malate in accessions of *Vitis* spp. of interest to grape breeders (*cinerea*, *riparia*) in comparison to *vinifera* and hybrid

cultivars, in hopes that insights from the study would aid in future molecular studies of the regulation of malate.

Development of flavor chemistry laboratory experiments for high school classes

A separate part of this dissertation research was to devise a series of flavor chemistry laboratory experiments for high school classes. Due to multiple serious injuries and incidents, chemistry experiments for secondary education are being re-examined for safety [41,42]. Although guidelines exist from national agencies on best practices [43], a major reason why these dangerous demonstrations persist is because they are spectacular and popular with students [44]. However, driven by a rising interest in food systems and food science spawned from popular culture media such as Morgan Spurlock's documentary film, Supersize Me, and food writers such as Michael Pollan, Samin Nosrat, and J. Kenji López-Alt, there have been several innovative strategies for incorporating food science into college undergraduate chemistry courses [45,46]. By comparison, lesson plans related to food science for the high school classroom are largely absent – especially those aligned with the recently released Next Generation Science Standards (NGSS) [47]. We have developed a safe, high school appropriate, and demonstration-rich lesson plan based on aroma and flavor chemistry in Chapter 4.

REFERENCES

[1] F. Dunemann, D. Ulrich, A. Boudichevskaia, C. Grafe, W.E. Weber, QTL mapping of aroma compounds analysed by headspace solid-phase microextraction gas chromatography in the apple progeny “Discovery” x “Prima,” Mol. Breed. 23 (2009) 501–521. doi:10.1007/s11032-008-9252-9.

[2] J. Vogt, D. Schiller, D. Ulrich, W. Schwab, F. Dunemann, Identification of lipoxygenase (LOX) genes putatively involved in fruit flavour formation in apple (Malus x domestica), Tree Genet. Genomes. 9 (2013) 1493–1511. doi:10.1007/s11295-013-0653-5.

[3] J.L. Rambla, A. Medina, A. Fernández-del-Carmen, W. Barrantes, S. Grandillo, M. Cammareri, G. López-Casado, G. Rodrigo, A. Alonso, S. García-Martínez, J. Primo, J.J. Ruiz, R. Fernández-Muñoz, A.J. Monforte, A. Granell, Identification, introgression, and validation of fruit volatile QTLs from a red-fruited wild tomato species, J. Exp. Bot. (2016) erw455. doi:10.1093/jxb/erw455.

[4] J. Battilana, L. Costantini, F. Emanuelli, F. Sevini, C. Segala, S. Moser, R. Velasco, G. Versini, M.S. Grando, The 1-deoxy-d-xylulose 5-phosphate synthase gene co-localizes with a major QTL affecting monoterpene content in grapevine, Theor. Appl. Genet. 118 (2009) 653–669. doi:10.1007/s00122-008-0927-8.

[5] J.M. Obando-Ulloa, J. Ruiz, A.J. Monforte, J.P. Fernández-Trujillo, Aroma profile of a collection of near-isogenic lines of melon (Cucumis melo L.), Food Chem. 118 (2010) 815–822. doi:10.1016/j.foodchem.2009.05.068.

[6] P.J. Martínez-García, D.E. Parfitt, E.A. Ogundiwin, J. Fass, H.M. Chan, R. Ahmad, S. Lurie, A. Dandekar, T.M. Gradziel, C.H. Crisosto, High density SNP mapping and QTL analysis for fruit quality characteristics in peach (Prunus persica L.), Tree Genet. Genomes. 9 (2013) 19–36. doi:10.1007/s11295-012-0522-7.

[7] A. Ben-Chaim, Y. Borovsky, M. Falise, M. Mazourek, B.C. Kang, I. Paran, M. Jahn, QTL analysis for capsaicinoid content in Capsicum, Theor. Appl. Genet. 113 (2006) 1481–1490. doi:10.1007/s00122-006-0395-y.

[8] Z. Migicovsky, S. Myles, Exploiting Wild Relatives for Genomics-assisted Breeding of Perennial Crops, Front. Plant Sci. 8 (2017) 1–16. doi:10.3389/fpls.2017.00460.

[9] D. Tieman, G. Zhu, M.F.R. Resende, T. Lin, C. Nguyen, D. Bies, J.L. Rambla, K.S.O. Beltran, M. Taylor, B. Zhang, H. Ikeda, Z. Liu, J. Fisher, I. Zemach, A. Monforte, D. Zamir, A. Granell, M. Kirst, S. Huang, H. Klee, A chemical genetic roadmap to improved tomato flavor, Science (80-.). 355 (2017) 391–394. doi:10.1126/science.aal1556.

[10] J. Zhang, J. Zhao, Y. Xu, J. Liang, P. Chang, F. Yan, M. Li, Y. Liang, Z. Zou, Genome-Wide Association Mapping for Tomato Volatiles Positively Contributing to Tomato Flavor, Front. Plant Sci. 6 (2015) 1–13. doi:10.3389/fpls.2015.01042.

[11] S. van Nocker, S.E. Gardiner, Breeding better cultivars, faster: applications of new technologies for the rapid deployment of superior horticultural tree crops, Hortic. Res. 1 (2014) 14022. doi:10.1038/hortres.2014.22.

[12] S. Yang, J. Fresnedo-Ramírez, M. Wang, L. Cote, P. Schweitzer, P. Barba, E.M. Takacs, M. Clark, J. Luby, D.C. Manns, G. Sacks, A.K. Mansfield, J. Londo, A. Fennell, D. Gadoury, B. Reisch, L. Cadle-Davidson, Q. Sun, A next-generation marker genotyping platform (AmpSeq) in heterozygous crops: a case study for marker-assisted selection in grapevine, Hortic. Res. 3 (2016) 16002. doi:10.1038/hortres.2016.2.
[13] H.J. Klee, D.M. Tieman, Genetic challenges of flavor improvement in tomato, Trends Genet. 29 (2013) 257–262. doi:10.1016/j.tig.2012.12.003.
[14] H.J. Klee, Improving the flavor of fresh fruits: genomics, biochemistry, and biotechnology, New Phytol. 187 (2010) 44–56.
[15] A. Doligez, E. Audiot, R. Baumes, P. This, QTLs for muscat flavor and monoterpenic odorant content in grapevine (Vitis vinifera L.), Mol. Breed. 18 (2006) 109–125. doi:10.1007/s11032-006-9016-3.
[16] B.I. Reisch, C.L. Owens, P.S. Cousins, Fruit breeding, in: M.L. Badenes, D.H. Byrne (Eds.), Fruit Breed., New York, 2012: pp. 225–262. doi:10.1007/978-1-4419-0763-9.
[17] L.F. Springer, G.L. Sacks, Protein-precipitable tannin in wines from Vitis vinifera and interspecific hybrid grapes (Vitis ssp.): Differences in concentration, extractability, and cell wall binding, J. Agric. Food Chem. 62 (2014) 7515–7523. doi:10.1021/jf5023274.
[18] L.F. Springer, R.W. Sherwood, G.L. Sacks, Pathogenesis-Related Proteins Limit the Retention of Condensed Tannin Additions to Red Wines, J. Agric. Food Chem. 64 (2016) 1309–1317. doi:10.1021/acs.jafc.5b04906.
[19] T.E. Acree, E.H. Lavin, R. Nishida, S. Watanabe, O-Amino Acetophenone the "Foxy" Smelling Component of Labruscana Grapes, in: Y. Bessiere, A.F. Thomas (Eds.), Flavour Sci. Technol. 6th Weurmann Symp., Wiley, Hoboken, 1990: pp. 49–52.
[20] Q. Sun, M.J. Gates, E.H. Lavin, T.E. Acree, G.L. Sacks, Comparison of odor-active compounds in grapes and wines from vitis vinifera and non-foxy American grape species, J. Agric. Food Chem. 59 (2011) 10657–10664. doi:10.1021/jf2026204.
[21] A.L. Waterhouse, G.L. Sacks, D.W. Jeffery, Understanding Wine Chemistry, Wiley, Chichester, 2016. doi:10.1002/9781118730720.
[22] W. Kliewer, Concentration of Tartrates, Malates, Glucose and Fructose in the Fruits of the Genus Vitis, Am. J. Enol. Vitic. 18 (1967) 87–96.
[23] C.T.M. Coquard Lenerz, Phenolic extraction from red hybrid winegrapes, 2012.
[24] A.C. Rice, Chemistry of Winemaking from Native American Grape Varieties, in: Chem. Winemak., 1974: pp. 88–115. doi:doi:10.1021/ba-1974-0137.ch004\r10.1021/ba-1974-0137.ch004.
[25] L.F. Springer, L.A. Chen, A.C. Stahlecker, P. Cousins, G.L. Sacks, Relationship of Soluble Grape-Derived Proteins to Condensed Tannin Extractability during Red Wine Fermentation, J. Agric. Food Chem. 64 (2016) 8191–8199. doi:10.1021/acs.jafc.6b02891.
[26] E.A. Souza-Silva, R. Jiang, A. Rodriguez-Lafuente, E. Gionfriddo, J. Pawliszyn, A critical review of the state of the art of solid-phase microextraction of complex

matrices I. Environmental analysis, TrAC - Trends Anal. Chem. 71 (2015) 224–235. doi:10.1016/j.trac.2015.04.016.
[27] É.A. Souza-Silva, E. Gionfriddo, J. Pawliszyn, A critical review of the state of the art of solid-phase microextraction of complex matrices II. Food analysis, TrAC - Trends Anal. Chem. 71 (2015) 236–248. doi:10.1016/j.trac.2015.04.018.
[28] J.L. Rambla, A. Trapero-Mozos, G. Diretto, A. Rubio-Moraga, A. Granell, L. Gómez-Gómez, O. Ahrazem, Gene-Metabolite Networks of Volatile Metabolism in Airen and Tempranillo Grape Cultivars Revealed a Distinct Mechanism of Aroma Bouquet Production, Front. Plant Sci. 7 (2016). doi:10.3389/fpls.2016.01619.
[29] C.M. Kalua, P.K. Boss, Sample preparation optimization in wine and grapes: Dilution and sample/headspace volume equilibrium theory for headspace solid-phase microextraction, J. Chromatogr. A. 1192 (2008) 25–35. doi:10.1016/j.chroma.2008.03.053.
[30] J.L. Rambla, C. Alfaro, A. Medina, M. Zarzo, J. Primo, A. Granell, Tomato fruit volatile profiles are highly dependent on sample processing and capturing methods, Metabolomics. 11 (2015) 1708–1720. doi:10.1007/s11306-015-0824-5.
[31] Y. Bezman, F. Mayer, G.R. Takeoka, R.G. Buttery, G. Ben-oliel, H.D. Rabinowitch, M. Naim, Differential effects of tomato (Lycopersicon esculentum Mill) matrix on the volatility of important aroma compounds, J. Agric. Food Chem. 51 (2003) 722–726. doi:10.1021/jf020892h.
[32] P. Schieberle, R.J. Molyneux, Quantitation of Sensory-Active and Bioactive Constituents of Food: A Journal of Agricultural and Food Chemistry Perspective, J. Agric. Food Chem. 60 (2012) 2404–2408. doi:10.1021/jf2047477.
[33] V. Canuti, M. Conversano, M.L. Calzi, H. Heymann, M.A. Matthews, S.E. Ebeler, Headspace solid-phase microextraction-gas chromatography-mass spectrometry for profiling free volatile compounds in Cabernet Sauvignon grapes and wines, J. Chromatogr. A. 1216 (2009) 3012–3022. doi:10.1016/j.chroma.2009.01.104.
[34] L.L. Haggerty, Ripening profile of grape berry acids and sugars in university of Minnesota wine grape cultivars, select Vitis vinifera, and other hybrid cultivars, University of Minnesota, 2013.
[35] H.W. Berg, M. Akiyoshi, The utility of potassium bitartrate concentration-product values in wine processing, Am. J. Enol. Vitic. 22 (1971) 127–134.
[36] H. Volschenk, H.J.J. van Vuuren, M. Viljoen-Bloom, Malic Acid in Wine: Origin, Function and Metabolism during Vinification, South African J. Enol. Vitic. 27 (2006) 123–136. doi:10.21548/27-2-1613.
[37] P.G. Iland, B.G. Coombe, Malate , Tartrate , Potassium , and Sodium in Flesh and Skin of Shiraz Grapes During Ripening : Concentration and Compartmentation, Am. J. Enol. Vitic. 39 (1988) 71–76.
[38] C. Sweetman, L.G. Deluc, G.R. Cramer, C.M. Ford, K.L. Soole, Regulation of malate metabolism in grape berry and other developing fruits, Phytochemistry. 70 (2009) 1329–1344. doi:10.1016/j.phytochem.2009.08.006.

[39] S. Yang, J. Fresnedo-Ramírez, Q. Sun, D.C. Manns, G.L. Sacks, A.K. Mansfield, J.J. Luby, J.P. Londo, B.I. Reisch, L.E. Cadle-Davidson, A.Y. Fennell, Next generation mapping of enological traits in an F2 interspecific grapevine hybrid family, PLoS One. 11 (2016) 1–19. doi:10.1371/journal.pone.0149560.
[40] J. Chen, N. Wang, L.C. Fang, Z.C. Liang, S.H. Li, B.H. Wu, Construction of a high-density genetic map and QTLs mapping for sugars and acids in grape berries, BMC Plant Biol. 15 (2015) 1–14. doi:10.1186/s12870-015-0428-2.
[41] K. Roy, Safer Science: Better Practices for Safety Issues in the Science Classroom and Laboratory, Sci. Teach. (2016) 56.
[42] J. Kemsley, Improving Chemistry Demonstration Safety, Chem. Eng. News. 92 (2014) 38.
[43] Chemical Safety for Teachers and Their Supervisors, Grades 7–12, American Chemiscal Society, ACS Board-Council Committee on Chemical Safety, Washington, D.C., 2001.
[44] J. Kemsley, How To Make Chemistry Classroom Demonstrations And Experiments Safer, Chem. Eng. News. 93 (2015) 37–39.
[45] P. Bell, Design of a Food Chemistry-Themed Course for Nonscience Majors, J. Chem. Educ. 91 (2014) 1631–1636. doi:10.1021/ed4003404.
[46] D.T. Miles, A.C. Borchardt, Laboratory Development and Lecture Renovation for a Science of Food and Cooking Course, J. Chem. Educ. 91 (2014) 1637–1642. doi:10.1021/ed5003256.
[47] NGSS Lead States, Next Generation Science Standards: For States, By States, (2013). https://www.nextgenscience.org/ (accessed January 1, 2019).

CHAPTER 2

HS-SPME-GC-MS ANALYSIS OF VOLATILES IN PLANTE POPULATIONS – QUANTITATING COMPOUND × INDIVIDUAL MATRIX EFFECTS

ABSTRACT

Headspace solid-phase microextraction (HS-SPME) coupled to gas chromatography–mass spectrometry (GC-MS) is widely employed for volatile analyses of plants, including mapping populations used in plant breeding research. Studies often employ a single internal surrogate standard, even when multiple analytes are measured, with the assumption that any relative changes in matrix effects among individuals would be similar for all compounds, i.e., matrix effects do not show Compound × Individual interactions. We tested this assumption using individuals from two plant populations: an interspecific grape (*Vitis* spp.) mapping population (n = 140) and a tomato (*Solanum* spp.) recombinant inbred line (RIL) population (n = 148). Individual plants from the two populations were spiked with a cocktail of internal standards (n = 6, 9, respectively) prior to HS-SPME-GC-MS. Variation in the relative responses of internal standards indicated that Compound × Individual interactions exist but were different between the two populations. For the grape population, relative responses among pairs of internal standards varied considerably among individuals, with a maximum of 249% relative standard deviation (RSD) for the pair of [U^{13}C]hexanal and [U^{13}C]hexanol. However, in the tomato population, relative responses of internal standard pairs varied much less, with pairwise RSDs ranging from 8% to 56%. The

approach described in this paper could be used to evaluate the suitability of using surrogate standards for HS-SPME-GC-MS studies in other plant populations.

INTRODUCTION

Headspace solid-phase microextraction (HS-SPME) is widely employed to isolate and pre-concentrate volatiles prior to gas chromatography–mass spectrometry (GC-MS) analysis [1–4]. SPME has several advantages over other sample preparation techniques (e.g., solid-phase extraction or liquid–liquid extraction), including its avoidance of solvents, ease of automation, and small sample size requirements [5]. These features make SPME particularly well suited for studies that require analysis of a large number of samples, e.g., when evaluating plant populations used by breeders in investigating the genetic underpinnings of traits [6,7]. Mapping of genes or quantitative trait loci (QTLs) controlling volatiles—including those associated with aroma—has been reported in several plant species, including tomatoes [2], melons [8,9], apples [10,11], and grapes [12–14]. Plant volatile phenotyping is usually performed by GC-MS, for both targeted analyses of a small number of volatiles [15,16] and broader profiling of a large number of targeted or nontargeted volatiles ("metabolomics") [1,2,8–10,17].

A challenge associated with SPME, however, is its high susceptibility to matrix effects, including plant matrixes [18,19]. For example, for a range of volatiles, SPME-GC-MS responses were reported to decrease by 2- to 12-fold in a tomato matrix [15]. This decrease could arise from either competition on the SPME fiber or decreases in analyte volatility. Matrix effects could be compensated for through appropriate

calibration, most commonly through the use of well-matched and equilibrated internal standards. When available, the preferred choice for an internal standard is a stable isotope-labeled analogue of the target analyte, i.e., stable isotope dilution analysis (SIDA) [20]. This technique has been employed in grape mapping populations to identify candidate genes associated with monoterpene production ("muscat" aroma) [12] following a solid-phase extraction, and in basmati rice grains for phenotype 2-acetyl-1-pyrroline ("nutty" aroma) following SPME [21]. SIDA, however, is not employed in most volatile phenotyping studies of breeding populations, including those using SPME, likely due to the high cost or commercial unavailability of isotopically labeled standards [20]. The impracticality of SIDA is particularly severe for nontargeted studies, which may involve measurement of dozens of volatiles whose identity is unknown prior to analysis. Instead, it is common for SPME-based volatile phenotyping studies to use a single surrogate standard or to normalize responses to the total ion count. In this approach, it is assumed that the relative matrix effects on any given compound (analyte or standard) are consistent among individuals, i.e., relative differences in analyte concentrations are preserved. Knowledge of relative ratios of volatiles is still potentially useful, e.g., in QTL analyses to identify associated genetic markers for breeding purposes or identify likely metabolic networks. However, the assumption that matrix effects do not show Compound × Individual interactions in ostensibly similar samples is not always valid. For example, the relative response for an *n*-decane surrogate in soybean oil changed by up to 8-fold as compared to ^{13}C-labeled internal standards following thermal oxidation of the oil matrix [22]. Similarly, modest variations in ethanol content of model wines caused Compound × Individual

matrix effects across a range of volatiles [23]. These effects would not allow for accurate relative quantification based on a single surrogate standard.

Although the occurrence of Compound × Individual matrix effects during SPME analysis of plant populations can be assumed, the extent of such interactions has not been quantitated and routine approaches to their determination have not been described. Evaluating the extent of these interactions is becoming more important in plant breeding research due to a greater interest in improving fruit flavor, in comparison to the historic focus of plant breeding on improving yield, storage characteristics, and disease resistance [24]. Compound × Individual interactions could potentially be much smaller than variation from other sources, e.g., biological variability, in which case the error introduced from using a surrogate standard would be tolerable. To our knowledge, an approach to quantitate the extent of Compound × Individual matrix effects during HS-SPME-GC-MS analyses—including analyses of plant populations—has not been described, even though this phenomenon is well known among analytical chemists to exist [22,25]. We hypothesized that these effects could be evaluated by comparing the relative responses of multiple internal standards within a population. In this report, we describe our approach, and use it to evaluate the extent of Compound × Individual matrix effects in a grape mapping population and a tomato recombinant inbred line (RIL) population.

MATERIALS AND METHODS

Chemical Reagents and Standards

The following chemicals were purchased from Sigma-Aldrich (St. Louis, MO, USA): sodium phosphate mono- (≥99%) and di-basic (≥98%), methanol (≥99%; MeOH), ethylenediaminetetraacetic acid disodium salt dihydrate (EDTA; ≥99%), 2-octanone (≥98%), nonyl acetate (FCC), and 4-methyl-2-pentanol (≥98%). [$^2H_3$]eucalyptol (>95%; >99% isotopic purity), [$^2H_3$]methyl anthranilate (>95%; >99% isotopic purity), and [$^2H_2$]-(*E*)-2-hexenal (>90%; >99% isotopic purity) were purchased from aromaLAB (Planegg, Germany); [$^2H_3$]-3-isobutyl-2-methoxypyrazine (IBMP) (>98%; >99% isotopic purity), [$^2H_3$]-3-isoproyl-2-methoxypyrazine (IPMP) (>98%; >99% isotopic purity), [$^2H_4$]furfural (>99%; >99% isotopic purity), [$^2H_8$]naphthalene (>98%; >99% isotopic purity), and [$^2H_4$]4-ethyl phenol (99%; >98% isotopic purity) were purchased from C/D/N Isotopes (Pointe-Claire, QC, Canada); [$^2H_{10}$]benzophenone (>99%; >99% isotopic purity) was purchased from o2si Smart Solutions (Charleston, SC). A [U^{13}C] internal standard extract where the concentration of [U^{13}C]hexanal and [U^{13}C]hexanol was ca. 30 µg/mL in MeOH was prepared as described in Supplementary Information (Figure S1). Deionized distilled water (18 MΩ) was used for all experiments (EMD Millipore Advantage A10). For the grapes, a pH 7.0 buffer solution was prepared from 0.1 M sodium phosphate dibasic/0.1 M sodium phosphate monobasic. For the tomatoes, a pH 7.5 buffer solution was prepared from 0.1 M EDTA. Both were stored at 4 °C.

Sample Collection of Grapes and Tomatoes

Grape samples for matrix effect evaluations were obtained from a research vineyard where seedlings from the cross of "Horizon" × Illinois 547-1 (*V. rupestris* × *V. cinerea*) [27] were grown. These vines were developed by Bruce Reisch of the Horticulture

Section at the New York State Agricultural Experiment Station, Geneva, NY, USA. The population was planted in two phases (1991 and 1998) with 2.7 m spaces between rows and 1.2 m between vines. About 400 g of ripe berries were collected from each of the 140 progeny during the 2013 harvest. The bagged samples were transported on ice packs in coolers back to the research station, where they were immediately moved into −20 °C storage.

Tomato fruit samples were obtained from an RIL population (148 lines) derived from an interspecific cross between *Solanum lycopersicum* L. breeding line NC EBR-1 and *Solanum pimpinellifolium* L. accession LA2093 [36]. Three plants of each of the 148 RILs and their two parents were grown in an open field in Live Oak, FL, USA during the spring of 2015. Red-ripe fruits were harvested from each plant, and pericarp tissues of at least three fruits per plant were flash-frozen in liquid nitrogen the following day. Samples were ground to a fine powder with an IKA A11 analytical mill (IKA®-Works, Inc., Wilmington, NC, USA,) and stored in 50 mL centrifuge tubes at −80 °C for future analysis.

Sample Preparation of Grapes and Tomatoes

Standard sample processing approach for grapes: For each individual (n = 140), frozen berries were thawed for 10 min, and 150 g were destemmed and macerated for 60–90 s in a chilled 250 mL stainless steel Waring blender. Berry slurry (5 g per vial, done in duplicate) was immediately transferred to two amber 20 mL SPME vials prefilled with 3 g of NaCl. The pH 7 phosphate buffer (5 mL; 0.1 M) was added, along with 20 µL of [$U^{13}C$] internal standard extract where the concentration of [$U^{13}C$]hexanal and [$U^{13}C$]hexanol was ca. 30 µg/mL in MeOH, as well as 20 µL of [$^2H_3$]eucalyptol,

[$^2H_3$]methyl anthranilate [$^2H_3$]IBMP, and [$^2H_3$]IPMP, where concentrations were ca. 2 ng/mL, 20 ng/mL, 20 pg/mL, and 20 pg/mL, respectively.

Standard sample processing approach for tomatoes: Samples (n = 243, from 114 of the 148 lines) were prepared according to Tikunov et al. [37] with slight modifications. Briefly, 1.5 g of ground tomato fruit tissue was aliquoted from each 50 mL centrifuge tube into a precooled (dry ice) 15 mL centrifuge tube, and immediately placed back on dry ice and stored in −80 °C. Prior to the analysis, the samples were thawed in a 30 °C water bath for 2 min. Then, 1.5 mL of 100 mM EDTA solution was added to the 15 mL tube, and the tube was shaken vigorously. Subsequently, the slurry (~2 mL) was transferred to a 10 mL SPME vial containing 2.4 g $CaCl_2$. The internal standard cocktail was immediately added. The cocktail contained 2-octanone, nonyl acetate, 4-methyl-2-pentanol, [$^2H_2$]-(*E*)-2-hexenal, [$^2H_3$]IPMP, [$^2H_4$]furfural, [$^2H_8$]naphthalene, [$^2H_4$]4-ethyl phenol, and [$^2H_{10}$]benzophenone; all concentrations were ca. 1.25 µg/mL. Samples were tightly capped, vortexed, and stored at 4 °C for 24 h prior to analysis.

Analysis of Grape Volatiles by HS-SPME-GC-MS

Volatile quantification was performed via HS-SPME–GC–TOF–MS (Pegasus 4D, LECO Corp., St. Joseph, MI, USA). Although the instrument is capable of two-dimensional GC analyses, all work was carried out in 1-D GC mode with the modulator and secondary oven turned off. A 2 cm divinylbenzene/Carboxen®/polydimethylsiloxane (DVB/CAR/PDMS) fiber was used for all HS-SPME extractions, with an incubation temperature of 40 °C, a pre-extraction incubation time of 10 min, and 30 min for HS-SPME extraction. A split/splitless injector was used with a constant temperature of 250 °C. SPME injections were splitless with a

flow rate of 50 mL/min and purge time of 3 min. Helium was used as a carrier gas at a flow rate of 1.5 mL/min. The GC column was a DB-5 ms (30 m × 0.25 mm × 0.25 μm, Varian, Walnut Creek, CA). The initial GC oven temperature was 50 °C and held for 5 min, then ramped to 180 °C at 5 °C per min, then ramped to 240 °C at 15 °C per min and held at 240 °C for 15 min. The TOF–MS was operated in EI mode with an ionization energy of 70 eV. The electron multiplier was set to 1700 V. MS data from m/z = 20−400 was stored at 5 Hz. Data processing was carried out by the LECO ChromaTOF software. The qualifier ions were as follows: for [U^{13}C]hexanal, m/z 46, 60, 76, 88; for [U^{13}C]hexanol, m/z 60, 74, 90; for [$^{2}H_3$]eucalyptol, m/z 114, 142, 157; for [$^{2}H_3$]methyl anthranilate, m/z 95, 122, 154; for [$^{2}H_3$]IBMP, m/z 127, 154, 169; and for [$^{2}H_3$]IPMP, m/z 127, 140, 155. The quantifier ions for [U^{13}C]hexanal, [U^{13}C]hexanol, [$^{2}H_3$]eucalyptol, [$^{2}H_3$]methyl anthranilate, [$^{2}H_3$]IBMP, and [$^{2}H_3$]IPMP were m/z 76, 74, 157, 154, 127, and 140, respectively.

Analysis of Tomato Volatiles by HS-SPME-GC-MS

The same GC-TOF-MS instrument was used for tomato analyses. A 1 cm DVB/CAR/PDMS fiber was used for all HS-SPME extractions, with an incubation temperature of 50 °C, a pre-extraction incubation time of 5 min, and 30 min for HS-SPME extraction. A split/splitless injector was used with a constant temperature of 250 °C. SPME injections were splitless with a flow rate of 50 mL/min and purge time of 3 min. Helium was used as a carrier gas at a flow rate of 1 mL/min. The GC column was a CP-Sil 8 ms (30 m × 0.25 mm × 0.25 μm, Agilent, The Netherlands). The initial GC oven temperature was 45 °C and held 5 min, then ramped to 180 °C at 5 °C per min, then ramped to 280 °C at 25 °C per min and held at 280 °C for 5 min. The TOF-MS was

operated in EI mode with an ionization energy of 70 eV. The electron multiplier was set to 1700 V. MS data from *m*/*z* = 41−250 was stored at 5 Hz. Data processing was carried out by the LECO ChromaTOF software. The qualifier ions were as follows: for 2-octanone, *m*/*z* 43, 58, 71, 128; for nonyl acetate, *m*/*z* 43, 56, 70, 98, 126; for 4-methyl-2-pentanol, *m*/*z* 45, 69, 87; for [$^2H_2$]-(*E*)-2-hexenal, *m*/*z* 57, 71, 85, 100; for [$^2H_3$]IPMP, *m*/*z* 127, 140, 155; for [$^2H_4$]furfural, *m*/*z* 42, 70, 98, 100; for [$^2H_8$]naphthalene, *m*/*z* 108, 136; for [$^2H_4$]4-ethyl phenol, *m*/*z* 111, 126; and for [$^2H_{10}$]benzophenone, *m*/*z* 82, 110, 192. The quantifier ions were as follows: for 2-octanone, *m*/*z* 128; for nonyl acetate, *m*/*z* 43; for 4-methyl-2-pentanol, *m*/*z* 45; for [$^2H_2$]-(*E*)-2-hexenal, *m*/*z* 85; for [$^2H_3$]IPMP, *m*/*z* 140; for [$^2H_4$]furfural, *m*/*z* 100; for [$^2H_8$]naphthalene, *m*/*z* 136; for [$^2H_4$]4-ethyl phenol, *m*/*z* 111; and for [$^2H_{10}$]benzophenone, *m*/*z* 110.

Statistical Analyses

Within- and across-replicate errors were calculated for each standard using the following formula, where σ_x represents the standard deviation of the log transformed peak area:

$$\sigma_x = \sqrt{\frac{\sum_{i=1}^{N}(x_i - \overline{x})^2}{N}} \quad (1)$$

where $x_i = log\left[\frac{[Area]_{replicate\ 1\ of\ individual\ i}}{\frac{[Area]_{replicate\ 1}+[Area]_{replicate\ 2}}{2}}\right]$ of the *i*th individual in the population for within-replicate error ($\sigma_{x,within}$), $x_i = log\left[\frac{[Area]_{replicate\ 1\ of\ individual\ i}}{mean\ area\ of\ standard\ across\ sample\ population}\right]$ for across-replicate error ($\sigma_{x,across}$), and $\overline{x}$ = mean value of x_i for the population.

The pairwise matrix error ($\sigma_{standard\ 1,standard\ 2}$) for each pair of standards was calculated using the above formula for σ_x, where $x_i = log\left[\frac{[Area]_{standard\ 1}}{[Area]_{standard\ 2}}\right]$ and $\overline{x}$ = mean of

the log-normalized ratios for each pairwise comparison (n = 140, n = 243). These comparisons were performed on all the internal standards.

The relative standard deviation (RSD) was calculated from the error by the following formula: $RSD = (10^{\sigma_x} - 1) \times 100\%$ for $\sigma_{x,within}$, $\sigma_{x,across}$, and $\sigma_{standard\ 1,standard\ 2}$.

R Studio v 1.0.153 (R Studio, Boston, MA, USA) was used for statistical analysis; JMP v 12.0 (SAS Institute Inc., Cary, NC, USA) was used for data visualization.

RESULTS AND DISCUSSION

General Approach to Estimating Compound × Sample Interactions ($\sigma_{std\ 1,std\ 2}$) in Plant Populations

The purpose of this study was to (i) develop and apply a quantitative approach for estimating the extent of Compound × Individual interactions during HS-SPME analysis and (ii) examine the appropriateness of using a single surrogate standard for volatile profiling in a given matrix as compared to more accurate (and more tedious and expensive) methods such as recovery spikes and isotopically labeled standards. In brief, the approach is as follows:

1. Samples are spiked with a cocktail of internal standards prior to SPME-GC-MS analysis (Figure 1). In the present work, as we were studying plant populations, these standards were either isotopic analogues of plant-derived odorants, or non-labeled surrogate standards previously reported for use in plant volatile profiling.

2. Pairwise matrix error ($\sigma_{std\ 1,std\ 2}$) is calculated as described in the Methods section and Figure 1, where the Compound × Individual interaction is assessed across a population for each internal standard, and quantified by the $\sigma_{std\ 1,std\ 2}$ value.

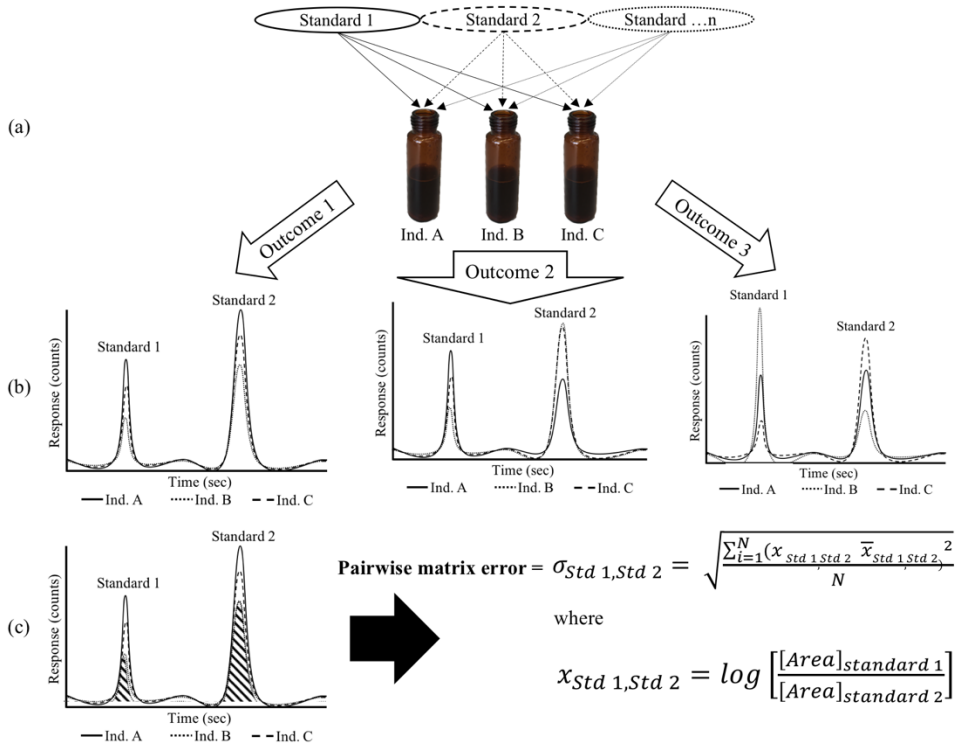

Figure 2.1: Overview of the experimental design.

(a) Multiple non-native internal standards were added to each plant individual during sample preparation. (b) Samples were analyzed by HS-SPME-GC-MS (simulated data shown). In some cases, pairs of standards had similar relative ratios across multiple individuals (Outcome 1), while in other cases there was evidence of Compound × Individual matrix effects, in which the relative peak areas for pairs of standards changed among individuals (Outcomes 2 and 3). (**c**) Compound × Individual matrix

effects were quantitated by comparing the log-transformed integrated peak areas for each standards pair using the pairwise matrix error formula ($\sigma_{std\ 1,std\ 2}$) described in the Methods section.

As proof of principle of the approach, we evaluated two plant populations where genome sequencing has been performed and for which there is interest in understanding the biochemical pathways responsible for regulating plant health, i.e., resistance to biotic and abiotic stress, as well as fruit quality [26]: (i) a *Vitis* spp. grape population ("Horizon" × Illinois 547-1) that had recently been genotyped using next-generation sequencing (NGS) approaches [7,27], and (ii) a tomato RIL population, which was recently genotyped by using the GBS (genotyping by sequencing) method [28] and evaluated using a single internal standard (Gonda et al., in preparation). While this approach yielded good results in a melon population [29], it is possible to discover better QTLs with better-matched internal standards.

Quantitating Compound × Individual Matrix Effects in a Grape Population

In initial inspection of our HS-SPME-GC-MS dataset, we observed good reproducibility of internal standard peak areas for analytical replicates from the same grape individual ($\sigma_{x,within}$); precisions ranged over RSD = 12–20% for all volatiles except for [U^{13}C]hexanal = 32% (data not shown). This range for precision is comparable to those in previous literature reports using HS-SPME-GC-MS on grape volatiles [30]. The presence of Compound × Individual interactions in the grape population is illustrated by three representative chromatograms, each depicting the behavior of a different compound pair across three individuals (Figure 2). For certain compound pairs, the variation in matrix effects is well correlated, e.g., for [$^{2}H_3$]IBMP

and [$^{2}H_3$]IPMP, Figure 2 (top). Although the signal is ~50% higher in Individual C than in Individual A for [$^{2}H_3$]IPMP, a similar change is seen for [$^{2}H_3$]IBMP; thus, the two compounds could serve as surrogate standards. In contrast, the relative responses of other compound pairs ([$^{2}H_3$]eucalyptol and [$^{2}H_3$]methyl anthranilate, Figure 2 (middle); and [U^{13}C]hexanal and [U^{13}C]hexanol, Figure 2 (bottom)) were not consistent. For example, the [$^{2}H_3$]methyl anthranilate signal was 4-fold higher in Individual A than in Individual B, but the [$^{2}H_3$]eucalyptol signal was nearly unchanged.

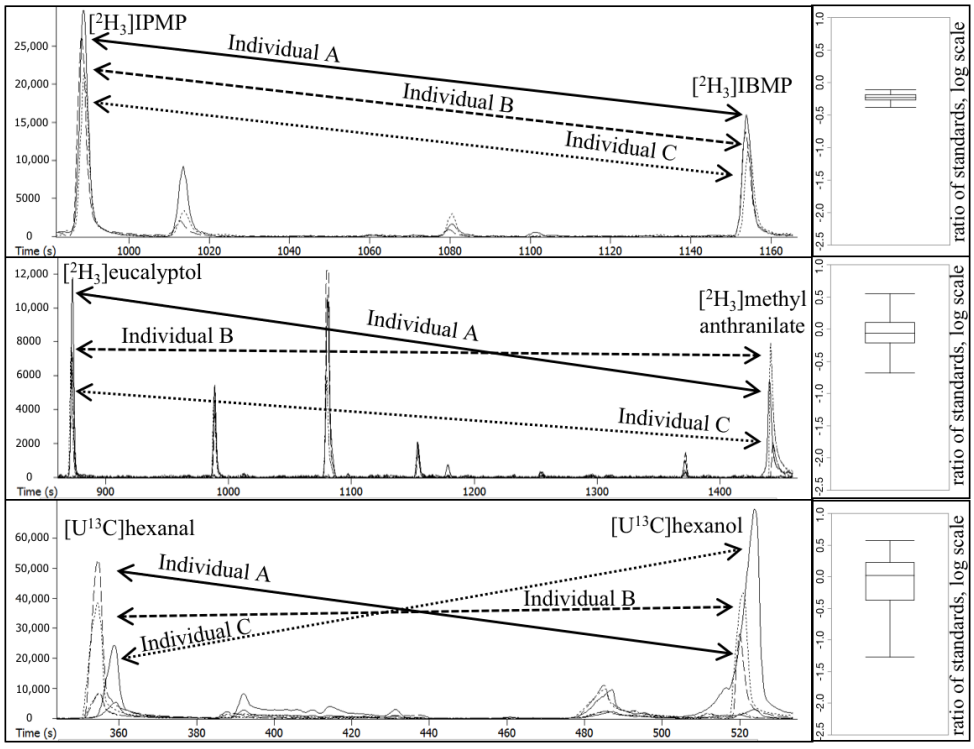

Figure 2.2: Chromatograms (left) and corresponding box plots (right) of Compound × Individual matrix effects for three pairs of internal standards in three different grape individuals (A, B, C). Internal standards are [$^{2}H_3$]IBMP and [$^{2}H_3$]IPMP (top), [$^{2}H_3$]eucalyptol and [$^{2}H_3$]methyl anthranilate (middle), and [U^{13}C]hexanal and [U^{13}C]hexanol (bottom).

In our analyses, samples were prepared and run in batches of up to 30 runs. Since a run length was approximately 60 min, including oven cooling time, some samples would have sat for up to 30 hours before analysis. Although we used brine addition to disrupt enzymatic activity and randomized the order of analyses, we were still concerned that variation in the signal could have arisen from nonenzymatic reactions or residual enzymatic activity. To evaluate this possibility, regression analyses of peak area versus run number were performed for each standard. Representative plots for [U^{13}C]hexanal and [U^{13}C]hexanol are shown in Supplementary Figure S2; other plots are not shown. With the exception of [U^{13}C]hexanal ($p = 0.01$, $r^2 = 0.18$), no significant effect of run number was observed for any of the internal standards. The effect of run number on [U^{13}C]hexanal was negative (decreasing signal intensity over time), and we observed that eliminating the first five vials of each batch from the ANOVA resulted in no significant correlation between run number and signal ($p > 0.05$, data not shown). The higher [U^{13}C]hexanal response in earlier runs was not due to instability of the standard under aqueous conditions—we observed no change in [U^{13}C]hexanal in a model juice system over 48 h (data not shown), nor was an increase observed for [U^{13}C]hexanol during later runs (Supplementary Figure S2). An alternate explanation for the higher [U^{13}C]hexanal in the first few runs of each batch is that the compound reacted with other nucleophilic juice components (e.g., polyphenols) [31]. Regardless of the cause, the effect of pre-analysis time explained only a small portion of the total variation observed in the [U^{13}C]hexanal response among individuals.

To quantitate Compound × Individual matrix effects ($\sigma_{std\ 1,std\ 2}$) we used the approach described in the previous subsection and outlined in Figure 1. Summary statistics are shown for each compound pair (Figure 3), where the percent relative standard deviation was calculated from the log-normalized pairwise matrix error. The pairwise matrix error for any two compounds will approach zero assuming that the compounds have minimal Compound × Individual matrix effects. Pairwise errors ranged from 17% to 249% for the 15 possible pairwise combinations. The smallest pairwise error (17%) was observed for [$^2H_3$]IPMP and [$^2H_3$]IBMP. This error is only modestly worse than precisions reported for 200 pg/g spikes of unlabeled IBMP and IPMP in Cabernet franc grape matrixes, quantified against [$^2H_3$]IBMP, which had % CVs of 2–8% [32]. IBMP and IPMP are homologues differing only by the presence of an additional -CH_2- group in IBMP, and thus are expected to share similar chemical properties. Thus, it is unsurprising that the pairwise matrix error is small. However, the pairwise matrix error was considerably worse for most of the other labeled analyte pairs. For example, the RSD associated with [$^2H_3$]methyl anthranilate quantified by [$^2H_3$]eucalyptol, [$^2H_3$]IBMP, or [$^2H_3$]IPMP ranged from 83 to 97%, while the minimum RSD associated with quantifying a compound by either [U^{13}C]hexanal or [U^{13}C]hexanol was 83% and rose to 249% when quantifying [U^{13}C]hexanal with [U^{13}C]hexanol. Interestingly certain combinations have low pairwise errors in spite of having different functional groups, e.g., [$^2H_3$]eucalyptol had low error (28–29%) when paired with either [$^2H_3$]IBMP or [$^2H_3$]IPMP.

Quantifying Compound × Individual Matrix Effects in a Tomato RIL Population

We trialed our approach with a tomato RIL population spiked with nine internal standards. This tomato population was selected because it had previously undergone volatile profiling using a single, non-native internal standard (2-octanone) [2]. The pairwise matrix error ranged from 8% to 56% among the 36 standard pairs evaluated (Figure 4). As with the grape population, compound pairs that showed the greatest differences in response across individuals (high values for $\sigma_{std\ 1,std\ 2}$) were not readily predictable from their chemistry. For example, it has been previously reported that volatiles with aromatic rings could participate in π-π interactions, decreasing their SPME response [33]. We therefore expected that internal standards with aromatic rings (e.g., [$^2H_4$]-4-ethyl phenol) should exhibit more correlated responses across individuals (lower $\boldsymbol{\sigma_{std\ 1,std\ 2}}$ values) than with nonaromatic standards. However, we observed that [$^2H_4$]-4-ethyl phenol showed similar (and relatively high) pairwise variation with respect to both straight-chain compounds (2-octanone, nonyl acetate; $\boldsymbol{\sigma_{std\ 1,std\ 2}}$ = 37-48%) and other aromatic compounds ([$^2H_8$]naphthalene, [$^2H_{10}$]benzophenone, [$^2H_3$]IPMP; $\boldsymbol{\sigma_{std\ 1,std\ 2}}$ = 42–49%). Conversely, [$^2H_3$]IPMP showed similar matrix effects with both a mid-chain branched alcohol (4-methyl-2-pentanol; $\boldsymbol{\sigma_{std\ 1,std\ 2}}$ = 15%) and the polyaromatic [$^2H_8$]naphthalene ($\boldsymbol{\sigma_{std\ 1,std\ 2}}$ = 8%). Overall, Compound × Individual matrix effects in the tomato population were considerably less than those observed in the grape population, with $\boldsymbol{\sigma_{std\ 1,std\ 2}}$ values ranging from 8% to 56%. Even at the extreme case of mismatched standards ([$^2H_4$]-4-ethylphenol vs [$^2H_4$]furfural or [$^2H_2$]-(*E*)-2-hexenal), the extent of the error ($\boldsymbol{\sigma_{std\ 1,std\ 2}}$ = 56%) may still be tolerable for many studies. The reason why Compound ×

Individual matrix effects occur to a lesser extent in the tomato population as compared to the grape population in our study is unclear, and further research is needed to determine if this is a general phenomenon or specific to this population.

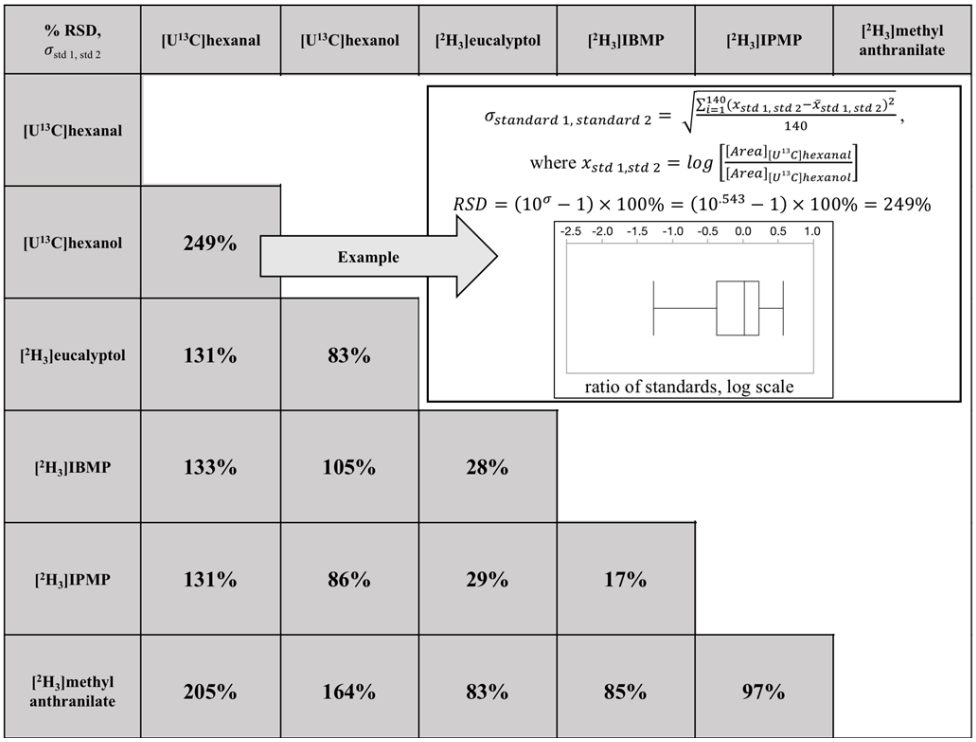

Figure 2.3: Compound × Individual matrix effects (%RSD) for pairs of six isotopically labeled internal standards in a grape population.

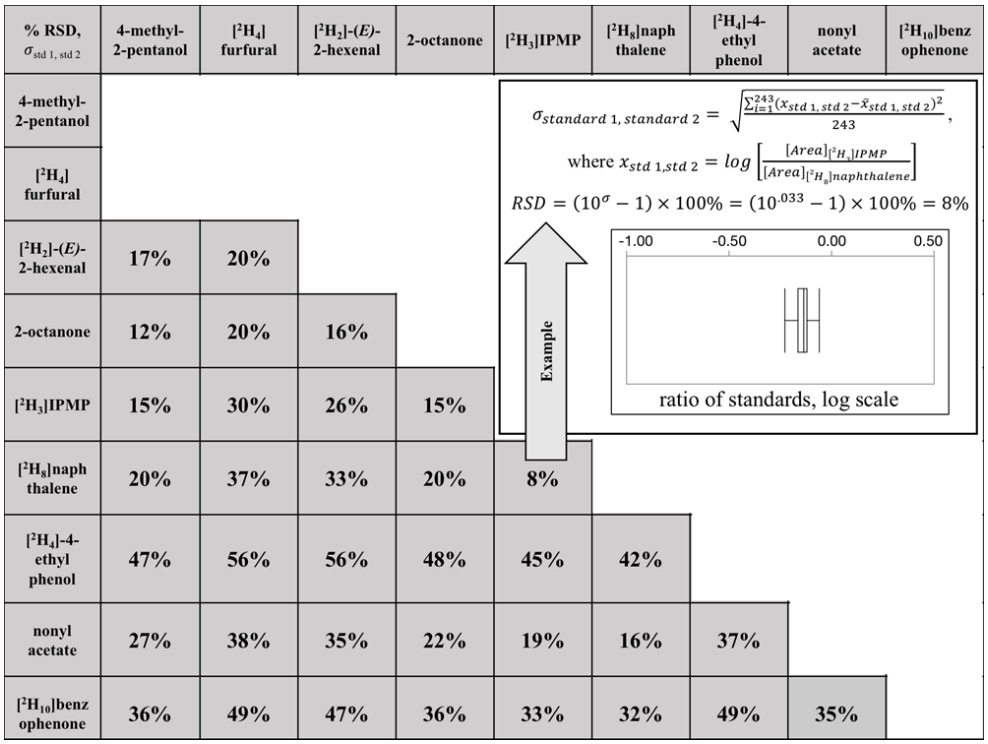

Figure 2.4: Compound × Individual matrix effects (%RSD) for pairs of nine non-native internal standards in a tomato population.

Consequences of Compound × Individual Matrix Effects within Plant Populations

The sample matrix is well known to affect HS-SPME recovery, either through competition on the SPME fiber, or through altering the volatility of analytes [5]. A less-appreciated problem is that HS-SPME matrix effects can show Compound × Individual interactions, which will affect the accuracy of even semiquantitative analyses (relative responses). Using our novel approach (Figure 1) we quantitated the extent of such interactions; pairwise errors arising from Compound × Individual matrix effects ranged from 17% to 249% among the 15 standard pairs evaluated in a grape population (Figure 3) and from 8% to 56% among the 36 standard pairs in a tomato population (Figure 4). In the worst-case scenario for either population (RSD = 249%), the 95% confidence interval would extend over 2 orders of magnitude. In situations where large, qualitative

variations in a trait are observed, these effects will likely be tolerable. For example, floral-smelling monoterpenes are up to 1000-fold higher in Muscat-type grapes as compared to non-Muscat grapes [12], and the trait is under the control of a single major locus (*VvDXS*). However, many volatiles in grapes (and other plants) vary over a more limited range. For example, IBMP concentrations are reported to range from <1 ng/L to 55 ng/L in wines produced from cultivars containing methoxypyrazines [34]. In these cases, a considerable portion of observed variation could arise from matrix effects rather than from real differences among samples, and the use of a poorly matched surrogate standard would likely obscure real differences. Although these issues could be addressed through approaches such as the use of isotopologues (stable isotope dilution analysis, SIDA), these standards are often expensive, challenging to synthesize, and/or not widely available [35]. Furthermore, the use of labeled standards requires that targets be identified prior to analysis, and therefore would not be appropriate for nontargeted studies in which analytes are identified post hoc. A key contribution of the approach described in this paper is that it allows for a quantitative estimate of the likely error associated with using a limited number of surrogate standards within a given matrix, and allows a researcher to determine if SIDA or other more involved approaches (e.g., recovery spikes) are advisable. Finally, although the work in this paper was limited to two plant populations, the approach should be broadly applicable to any study with many individual samples.

Conclusions

We have reported an approach to estimating the extent of Compound × Individual matrix effects during volatile analyses. In this approach, the variances of the ratios of

non-native standard pairs are determined, and the range of these values establishes the error expected from using a single surrogate standard during volatile analyses. This report specifically focused on the use of HS-SPME-GC-MS for the characterization of volatiles in plant populations (tomato and grape), although the approach should be equally appropriate for application to other analytical techniques or populations. We observed much greater Compound × Individual matrix effects for compound pairs in the grape population, with RSD = 249% for the pair of hexanal and hexanol. We also observed that the best surrogate standard for a given compound could not be easily predicted from the chemical structures of the compound. Based on these results, in situations where surrogate standards are used in HS-SPME-GC-MS analyses, we recommend characterizing the extent of Compound × Individual matrix effects to confirm that these effects are small in comparison to the desired accuracy.

REFERENCES

1. Rambla, J.L.; Trapero-Mozos, A.; Diretto, G.; Rubio-Moraga, A.; Granell, A.; Gómez-Gómez, L.; Ahrazem, O. Gene-Metabolite Networks of Volatile Metabolism in Airen and Tempranillo Grape Cultivars Revealed a Distinct Mechanism of Aroma Bouquet Production. *Front. Plant Sci.* **2016**, *7*, doi:10.3389/fpls.2016.01619.
2. Zhang, J.; Zhao, J.; Xu, Y.; Liang, J.; Chang, P.; Yan, F.; Li, M.; Liang, Y.; Zou, Z. Genome-Wide Association Mapping for Tomato Volatiles Positively Contributing to Tomato Flavor. *Front. Plant Sci.* **2015**, *6*, 1–13, doi:10.3389/fpls.2015.01042.
3. Slegers, A.; Angers, P.; Ouellet, É.; Truchon, T.; Pedneault, K. Volatile compounds from grape skin, juice and wine from five interspecific hybrid grape cultivars grown in Québec (Canada) for wine production. *Molecules* **2015**, *20*, 10980–11016, doi:10.3390/molecules200610980.
4. Ma, X.-W.; Su, M.-Q.; Wu, H.-X.; Zhou, Y.-G.; Wang, S.-B. Analysis of the Volatile Profile of Core Chinese Mango Germplasm by Headspace Solid-Phase Microextraction Coupled with Gas Chromatography-Mass Spectrometry. *Molecules* **2018**, *23*, 1480, doi:10.3390/molecules23061480.
5. Marsili, R. *Flavor, Fragrance, and Odor Analysis*, 2nd ed.;CRC Press: Boca Raton, FL, USA, 2012.
6. van Nocker, S.; Gardiner, S.E. Breeding better cultivars, faster: applications of new technologies for the rapid deployment of superior horticultural tree crops. *Hortic. Res.* **2014**, *1*, 14022, doi:10.1038/hortres.2014.22.
7. Yang, S.; Fresnedo-Ramírez, J.; Wang, M.; Cote, L.; Schweitzer, P.; Barba, P.; Takacs, E.M.; Clark, M.; Luby, J.; Manns, D.C.; et al. A next-generation marker genotyping platform (AmpSeq) in heterozygous crops: a case study for marker-assisted selection in grapevine. *Hortic. Res.* **2016**, *3*, 16002, doi:10.1038/hortres.2016.2.
8. Chaparro-Torres, L.A.; Bueso, M.C.; Fernández-Trujillo, J.P. Aroma volatiles obtained at harvest by HS-SPME/GC-MS and INDEX/MS-E-nose fingerprint discriminate climacteric behaviour in melon fruit. *J. Sci. Food Agric.* **2016**, *96*, 2352–2365, doi:10.1002/jsfa.7350.
9. Obando-Ulloa, J.M.; Ruiz, J.; Monforte, A.J.; Fernández-Trujillo, J.P. Aroma profile of a collection of near-isogenic lines of melon (*Cucumis melo* L.). *Food Chem.* **2010**, *118*, 815–822, doi:10.1016/j.foodchem.2009.05.068.
10. Dunemann, F.; Ulrich, D.; Boudichevskaia, A.; Grafe, C.; Weber, W.E. QTL mapping of aroma compounds analysed by headspace solid-phase microextraction gas chromatography in the apple progeny "Discovery" × "Prima." *Mol. Breed.* **2009**, *23*, 501–521, doi:10.1007/s11032-008-9252-9.
11. Vogt, J.; Schiller, D.; Ulrich, D.; Schwab, W.; Dunemann, F. Identification of lipoxygenase (LOX) genes putatively involved in fruit flavour formation in apple (Malus × domestica). *Tree Genet. Genomes* **2013**, *9*, 1493–1511, doi:10.1007/s11295-013-0653-5.
12. Battilana, J.; Costantini, L.; Emanuelli, F.; Sevini, F.; Segala, C.; Moser, S.; Velasco, R.; Versini, G.; Grando, M.S. The 1-deoxy-d-xylulose 5-phosphate

synthase gene co-localizes with a major QTL affecting monoterpene content in grapevine. *Theor. Appl. Genet.* **2009**, *118*, 653–669, doi:10.1007/s00122-008-0927-8.
13. Doligez, A.; Audiot, E.; Baumes, R.; This, P. QTLs for muscat flavor and monoterpenic odorant content in grapevine (*Vitis vinifera* L.). *Mol. Breed.* **2006**, *18*, 109–125, doi:10.1007/s11032-006-9016-3.
14. Guillaumie, S.; Ilg, A.; Réty, S.; Brette, M.; Trossat-Magnin, C.; Decroocq, S.; Léon, C.; Keime, C.; Ye, T.; Baltenweck-Guyot, R.; et al. Genetic Analysis of the Biosynthesis of 2-Methoxy-3-Isobutylpyrazine, a Major Grape-Derived Aroma Compound Impacting Wine Quality. *Source Plant Physiol.* **2013**, *162*, 604–615.
15. Bezman, Y.; Mayer, F.; Takeoka, G.R.; Buttery, R.G.; Ben-oliel, G.; Rabinowitch, H.D.; Naim, M. Differential effects of tomato (Lycopersicon esculentum Mill) matrix on the volatility of important aroma compounds. *J. Agric. Food Chem.* **2003**, *51*, 722–726, doi:10.1021/jf020892h.
16. Vandendriessche, T.; Nicolai, B.M.; Hertog, M.L.A.T.M. Optimization of HS SPME Fast GC-MS for High-Throughput Analysis of Strawberry Aroma. *Food Anal. Methods* **2013**, *6*, 512–520, doi:10.1007/s12161-012-9471-x.
17. García-Vico, L.; Belaj, A.; Sánchez-Ortiz, A.; Martínez-Rivas, J.M.; Pérez, A.G.; Sanz, C. Volatile Compound Profiling by HS-SPME/GC-MS-FID of a Core Olive Cultivar Collection as a Tool for Aroma Improvement of Virgin Olive Oil. *Molecules* **2017**, *22*, 141, doi:10.3390/molecules22010141.
18. Souza-Silva, É.A.; Gionfriddo, E.; Pawliszyn, J. A critical review of the state of the art of solid-phase microextraction of complex matrices II. Food analysis. *TrAC–Trends Anal. Chem.* **2015**, *71*, 236–248, doi:10.1016/j.trac.2015.04.018.
19. Lloyd, N.; Johnson, D.L.; Herderich, M.J. Metabolomics approaches for resolving and harnessing chemical diversity in grapes, yeast and wine. *Aust. J. Grape Wine Res.* **2015**, *21*, 723–740, doi:10.1111/ajgw.12202.
20. Schieberle, P.; Molyneux, R.J. Quantitation of Sensory-Active and Bioactive Constituents of Food: A Journal of Agricultural and Food Chemistry Perspective. *J. Agric. Food Chem.* **2012**, *60*, 2404–2408, doi:10.1021/jf2047477.
21. Hopfer, H.; Jodari, F.; Negre-Zakharov, F.; Wylie, P.L.; Ebeler, S.E. HS-SPME-GC-MS/MS Method for the Rapid and Sensitive Quantitation of 2-Acetyl-1-pyrroline in Single Rice Kernels. *J. Agric. Food Chem.* **2016**, *64*, 4114–4120, doi:10.1021/acs.jafc.6b00703.
22. Gómez-Cortés, P.; Brenna, J.T.; Sacks, G.L. Production of isotopically labeled standards from a uniformly labeled precursor for quantitative volatile metabolomic studies. *Anal. Chem.* **2012**, *84*, 5400–5406, doi:10.1021/ac300933d.
23. Castro, R.; Natera, R.; Benitez, P.; Barroso, C.G. Comparative analysis of volatile compounds of "fino" sherry wine by rotatory and continuous liquid-liquid extraction and solid-phase microextraction in conjunction with gas chromatography-mass spectrometry. *Anal. Chim. Acta* **2004**, *513*, 141–150, doi:10.1016/j.aca.2004.02.002.
24. Klee, H.J.; Tieman, D.M. Genetic challenges of flavor improvement in tomato. *Trends Genet.* **2013**, *29*, 257–262, doi:10.1016/j.tig.2012.12.003.

25. Ferreira, V.; Herrero, P.; Zapata, J.; Escudero, A. Coping with matrix effects in headspace solid phase microextraction gas chromatography using multivariate calibration strategies. *J. Chromatogr. A* **2015**, *1407*, 30–41, doi:10.1016/j.chroma.2015.06.058.
26. Badenes, M.L.; Byrne, D.H. *Fruit breeding*; Springer Science & Business Media: Berlin, Germany, 2012; ISBN 9781441907639.
27. Hyma, K.E.; Barba, P.; Wang, M.; Londo, J.P.; Acharya, C.B.; Mitchell, S.E.; Sun, Q.; Reisch, B.; Cadle-Davidson, L. Heterozygous mapping strategy (HetMappS) for high resolution genotyping-by-sequencing markers: A case study in grapevine. *PLoS ONE* **2015**, *10*, 1–31, doi:10.1371/journal.pone.0134880.
28. Gonda, I.; Ashrafi, H.; Lyon, D.A.; Strickler, S.R.; Hulse-Kemp, A.M.; Ma, Q.; Sun, H.; Stoffel, K.; Powell, A.F.; Futrell, S.; et al. A GBS-based high-density genetic map of a tomato RIL population, facilitating high-resolution QTL mapping and candidate gene identification. *Plant Genome* **2018**, in press.
29. Galpaz, N.; Gonda, I.; Shem-Tov, D.; Barad, O.; Tzuri, G.; Lev, S.; Fei, Z.; Xu, Y.; Mao, L.; Jiao, C.; et al. Deciphering genetic factors that determine melon fruit-quality traits using RNA-Seq-based high-resolution QTL and eQTL mapping. *Plant J.* **2018**, *94*, 169–191, doi:10.1111/tpj.13838.
30. Canuti, V.; Conversano, M.; Calzi, M.L.; Heymann, H.; Matthews, M.A.; Ebeler, S.E. Headspace solid-phase microextraction-gas chromatography-mass spectrometry for profiling free volatile compounds in Cabernet Sauvignon grapes and wines. *J. Chromatogr. A* **2009**, *1216*, 3012–3022, doi:10.1016/j.chroma.2009.01.104.
31. Hidalgo, F.J.; Aguilar, I.; Zamora, R. Model Studies on the Effect of Aldehyde Structure on Their Selective Trapping by Phenolic Compounds. *J. Agric. Food Chem.* **2017**, *65*, 4736–4743, doi:10.1021/acs.jafc.7b01081.
32. Ryona, I.; Pan, B.S.; Sacks, G.L. Rapid measurement of 3-Alkyl-2-methoxypyrazine content of winegrapes to predict levels in resultant wines. *J. Agric. Food Chem.* **2009**, *57*, 8250–8257, doi:10.1021/jf9019695.
33. Aronson, J.; Ebeler, S.E. Effect of polyphenol compounds on the headspace volatility of flavors. *Am. J. Enol. Vitic.* **2004**, *55*, 13–21.
34. Dunlevy, J.; Kalua, C.; Keyzers, R.; Boss, P. The Production of Flavour & Aroma Compounds in Grape Berries. In *Grapevine Molecular Physiology & Biotechnology*; Roubelakis-Angelakis, K.A., Ed.; Springer: Dordrecht, The Netherland, 2009; pp. 293–340, ISBN 978-90-481-2304-9.
35. Souza-Silva, E.A.; Jiang, R.; Rodriguez-Lafuente, A.; Gionfriddo, E.; Pawliszyn, J. A critical review of the state of the art of solid-phase microextraction of complex matrices I. Environmental analysis. *TrAC–Trends Anal. Chem.* **2015**, *71*, 224–235, doi:10.1016/j.trac.2015.04.016.
36. Ashrafi, H.; Kinkade, M.; Foolad, M.R. A new genetic linkage map of tomato based on a Solanum lycopersicum × S. pimpinellifolium RIL population displaying locations of candidate pathogen response genes. *Genome* **2009**, *52*, 935–956, doi:10.1139/g09-065.

CHAPTER 3

MALATE CONTENT IN WILD *VITIS* SPP. DEMONSTRATES A RANGE OF BEHAVIORS DURING BERRY MATURATION

ABSTRACT

Wild *Vitis* spp. and their interspecific hybrids are known to have high malate concentrations at sugar maturity as compared to domesticated *vinifera*, but it is unknown if differences in malate at harvest among species arise from differences in malate accumulation or degradation. Over two years, fruit from *V. riparia* and *V. cinerea* accessions along with commercial *V. vinifera* and interspecific hybrid cultivars were collected at multiple time points. In contrast to the well-known biphasic behavior of malate in *vinifera* (pre-veraison accumulation, post-veraison degradation), we observed a range of behaviors for malate in wild species. On average, *riparia* accessions had malate per berry comparable to *vinifera* just prior to veraison, but degraded malate to a much lesser extent. *Cinerea* accessions had significantly lower malate prior to veraison than all other groups, but showed a post-veraison increase in malate. Variation in post-veraison malate behavior appears related to diminished malate degradation in the mesocarp of wild *Vitis spp*. Our results indicate that studies of malate behavior in *Vitis* spp. and their hybrids should include both pre- and post-veraison time points.

INTRODUCTION

Hybrids of domesticated European grapes and wild grape (*V. vinifera* × *Vitis* spp.) have several advantages over *V. vinifera*, such as improved cold hardiness and disease resistance (Reisch et al. 2012). However, these interspecific hybrids can yield wines with undesirable organoleptic properties, including excessive sourness (Rice 1974; Coquard Lenerz 2012). Sourness is well correlated with titratable acidity (TA) (Plane et al. 1980), and several wild *Vitis* spp., e.g. *V. riparia*, *V. rupestris*, and *V. cinerea,* can have TA approaching 50 g/L as tartaric acid equivalents even at normal levels of total soluble solids (TSS) for harvest-ripe grapes (TSS > 20 Brix) (Sun et al. 2011). These concentrations are considerably higher than the TA range of 6-9 g/L typically observed in mature *V. vinifera* (Waterhouse et al. 2016). The major organic acid in many wild *Vitis* spp. is malate, where it can be present at concentrations > 20 g/L in mature fruit (Kliewer et al. 1967). Similarly, interspecific hybrids are reported to have higher malate than their *V. vinifera* counterparts at harvest (5.0-7.3 g/L vs. 2.7-4.2 g/L), even when grown on the same site with similar cultural practices (Haggerty 2013). In winemaking, high malate in grapes is of greater concern than high concentrations of the other major grape acid (tartaric), as the latter generally has a limited concentration range in wines due to the low solubility of potassium bitartrate in hydroalcoholic solutions (Waterhouse et al. 2016). Remediation strategies for high malate, such as malolactic fermentation and ‘double-salt’ precipitation, are not appropriate for all wines and can still result in high TA even once complete (Waterhouse et al. 2016). Thus, producing hybrid grapes with lower malate is of

interest to the wine industry, either through use of appropriate viticultural practices or through breeding of new grape cultivars.

Malate exhibits a biphasic pattern in *vinifera* with initial accumulation in the vacuoles of immature fruit, primarily in the mesocarp (Iland and Coombe 1988). Starting at veraison, malate content decrease largely because berries switch from accumulating to degrading malate, and to a more limited extent because of dilution due to berry expansion (Sweetman et al. 2009). In contrast, the temporal pattern leading to the final malate content in berries of wild *Vitis* spp. and their hybrids has not been characterized, and mechanistic explanations for high malate have not been presented. Quantitative trait loci (QTL) analyses of *Vitis* spp. populations have been ambiguous – one study of a Seyval F_2 mapping population identified a weak QTL in a region containing a gene associated with an aluminum-activated malate transporter (ALMT) (Yang et al. 2016); another identified several minor QTLs for malate, but were unable to assign these to specific candidate genes (Chen et al. 2015). One limitation of these studies is the attempt to characterize this dynamic trait by the use of a single time-point, i.e., post-veraison, mature fruit, masking possible differences in the temporal pattern of malate. The goal of this research was to characterize the developmental profile of malate in accessions of *Vitis* spp. of interest to grape breeders (*cinerea*, *riparia*) in comparison to *vinifera* and hybrid cultivars, and will facilitate the testing of hypotheses in future molecular or empirical studies on the regulation of malate.

MATERIALS AND METHODS

Sample Collection and Preparation – Behavior of malate during ripening of Vitis spp.

V. riparia and *V. cinerea* grape clusters (~250 g) were collected from USDA-ARS Cold Hardy Grape Germplasm collection (Geneva, NY), and *V. vinifera* and interspecific hybrid samples were collected at Silver Thread Vineyards (Lodi, NY), and Swedish Hill Vineyards (Romulus, NY). Sampling took place on 03 Aug. 2015, 26 Aug. 2015, and 07 Oct. 2015 and between 09 Aug. 2016 and 05 Oct. 2016. For both 2015 and 2016, samplings were taken during the lag phase prior to veraison, and a subsequent 2-4 more samplings were taken until maximum ripeness, determined both by berry color and TSS, was achieved. Due to the asynchronous ripening across clusters and species, veraison was defined as the intermediate date between berry collection at all green color and at 100% color change per accession. This was further corroborated by TSS measurements at each sampling. For most cultivars, the final sampling point occurred at TSS associated with commercial maturity (> 20 Brix), although some late-maturing *V. cinerea* accessions did not reach this level. For 2015, in total, 103 samples were analyzed: 19 *V. cinerea* (7 accessions), 54 *V. riparia* (15 accessions), and 30 *V. vinifera* (5 cultivars). For 2016, 132 samples were collected: 59 *V. cinerea* (16 accessions), 35 *V. riparia* (10 accessions), 17 *V. vinifera* (3 cultivars), and 21 *Vitis* interspecific hybrids (4 cultivars). Wild *Vitis* accession numbers and interspecific hybrid and *V. vinifera* cultivar information are listed in Supplementary Table 1. All samples were frozen at -20 °C until processing. For sample preparation, 30 g of frozen berries selected at random were destemmed, counted, and weighed to determine mean berry weight. Berries were then thawed at room temperature for 20

min, macerated for 120 s in a chilled 250 mL stainless steel Waring blender, and strained through cheesecloth.

Sample Collection and Preparation – Distribution of malate between skin and mesocarp across Vitis spp.

V. riparia and *V. cinerea* grape clusters (~250 g) were collected from USDA-ARS Germplasm (Geneva, NY), and *V. vinifera* samples were collected from the Cornell Cooperative Extension (CCE) and Finger Lakes Community College (FLCC) teaching vineyard at Anthony Road Wine Co. (Penn Yan, NY). Sample list and basic fruit chemistry are included in Supp. Info., Table 1. Sampling took place at the onset of veraison in each genotype and ca. 30 days after, spanning between 14 Aug. 2018 and 31 Oct. 2018. All samples were frozen at -80 °C until processing. From each sample, a random subsample of 15 berries was taken and weighed. Berry dissection of skin, mesocarp, and seeds followed Iland and Coombe (1988), with slight modifications. Berries were placed on dry ice to keep the mesocarp frozen and limit the adhesion of cells to skin tissues. Berry skin was carefully peeled, patted dry on filter paper, and weighed. The remaining mesocarp and seeds were weighed and gently crushed to avoid seed damage. For extraction of water-soluble malate, berry mesocarp and seeds were combined with DDI water (approx. 2 × tissue mass in mL) and agitated in a parafilm-sealed 50 mL Erlenmeyer flask for 10 min, after which no further extraction of malate occurred (data not shown). One mL of extract was diluted 10-fold in DDI water for malate analysis. After extraction, seeds were wiped dry with a paper cloth and weighed.

Sample Characterization: Soluble Solids, pH, Malate

Total soluble solids and pH were measured on extracted juice by a digital refractometer (Sper Scientific, Ltd., model # 300053, Scottsdale, AZ) and pH meter (ThermoScientific, Orion 5 Star Series, Waltham, MA) respectively.

For malate, an enzymatic analysis method outlined in Zoecklein et al. (1999) was employed. For the survey of *Vitis* spp., malate was analyzed by an Agilent 8453 UV-vis spectrophotometer (Santa Clara, CA). Assay reagents (Glycine, hydrazine sulphate salt, NaOH, β-NAD, DL-malic acid, and malate dehydrogenase (2,770 U/mg protein, in ammonium sulfate suspension)) were purchased from Sigma Aldrich. For dissected tissues, malate was quantified using a ML 8343 UV-based malic acid kit on an RX Monaco autoanalyzer (Randox Laboratories Ltd.).

Statistical Analysis

Statistical tests were performed using JMP V.14 (SAS Institute Inc., Cary, NC). Malate measurements were natural-log transformed to normalize the data prior to analysis.

RESULTS AND DISCUSSION

Wild Vitis spp. show less malate degradation than vinifera

The behavior of malate in accessions of two wild species (*V. cinerea* and *V. riparia*) from a national germplasm collection were evaluated in comparison to domesticated *vinifera* and interspecific hybrids. These wild species were selected due to their importance to wine grape breeding programs, e.g. as a source of powdery mildew resistance (Fresnedo-Ramírez et al. 2017) and cold hardiness (Londo and Kovaleski

2017). TSS, pH, and malate content for all time points and cultivars/accessions are presented in Supplementary Table 1. Most accessions/cultivars reached TSS > 20 Brix, a level typically associated with commercial maturity in the Finger Lakes, although some late maturing *cinerea* accessions did not reach this level. Representative examples of malate content for each *Vitis* species as a function of maturity, defined as days post-veraison (dpv), are presented in Figure 1. The species bloomed and matured at different times, resulting in variation in the earliest and latest sampling points (in dpv) – however, all accessions were measured between approximately -15 to +15 dpv. *Vinifera* cultivars demonstrated the classical, biphasic pattern of malate accumulation before veraison, and an 80-90% decrease on a per berry basis post-veraison (Iland and Coombe 1988). In comparison, wild *Vitis* spp. also accumulated malate pre-veraison, but appeared to have negligible malate degradation post-veraison (Figure 1).

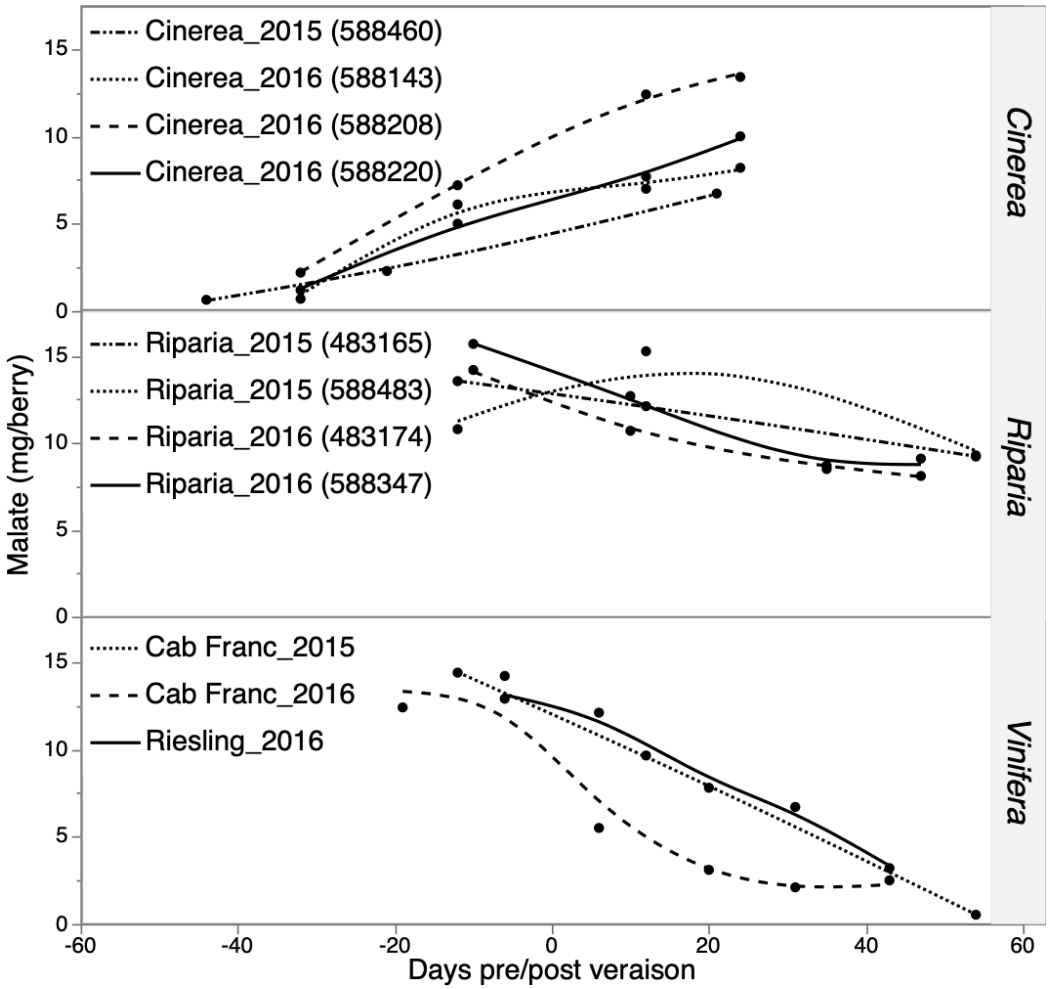

Figure 3.1: Representative examples of temporal patterns of malate behavior (mg/berry) as a function of days pre/post-veraison among *Vitis* spp.. Individual *cinerea* and *riparia* accession numbers are shown in parentheses.

To facilitate statistical analyses, we compared malate content per berry (Figure 2) at lag phase prior to color change (approximately -15 dpv for 2015 and -11 dpv for 2016) among species. Similar comparisons were performed for post-veraison samples at 15 dpv for 2015 and 19 dpv for 2016. As seen in Figure 2a and 2c, pre-veraison malate was significantly lower in *V. cinerea* (mean = 3.6 mg / berry for 2015; 5 mg / berry for

2016) than other species (*vinifera*, *riparia*, and interspecific; range = 9 – 16 mg / berry across the 2 years; Figure 2a and 2b, $p < 0.05$). At the post-veraison time point, there was no significant difference in the malate content among species (Figure 2b) in 2015. However, in 2016, malate content in *cinerea* and *riparia* was significantly greater than in *vinifera* and the interspecific hybrids ($p<0.05$) (Figure 2d). Similar statistical analyses were performed on malate concentrations (w/v) at pre and post-veraison time points (Figure 3). Differences in pre-veraison malate concentrations among species were not consistent across 2015 and 2016, although *V. riparia* was in the highest concentration grouping for both years (mean = 21-25 g/L) (Fig. 3a and 3c). At the post-veraison time points, malate concentrations followed the order of *cinerea* > *riparia* > *vinifera* and hybrids ($p < 0.05$) (Fig. 3b and 3d).

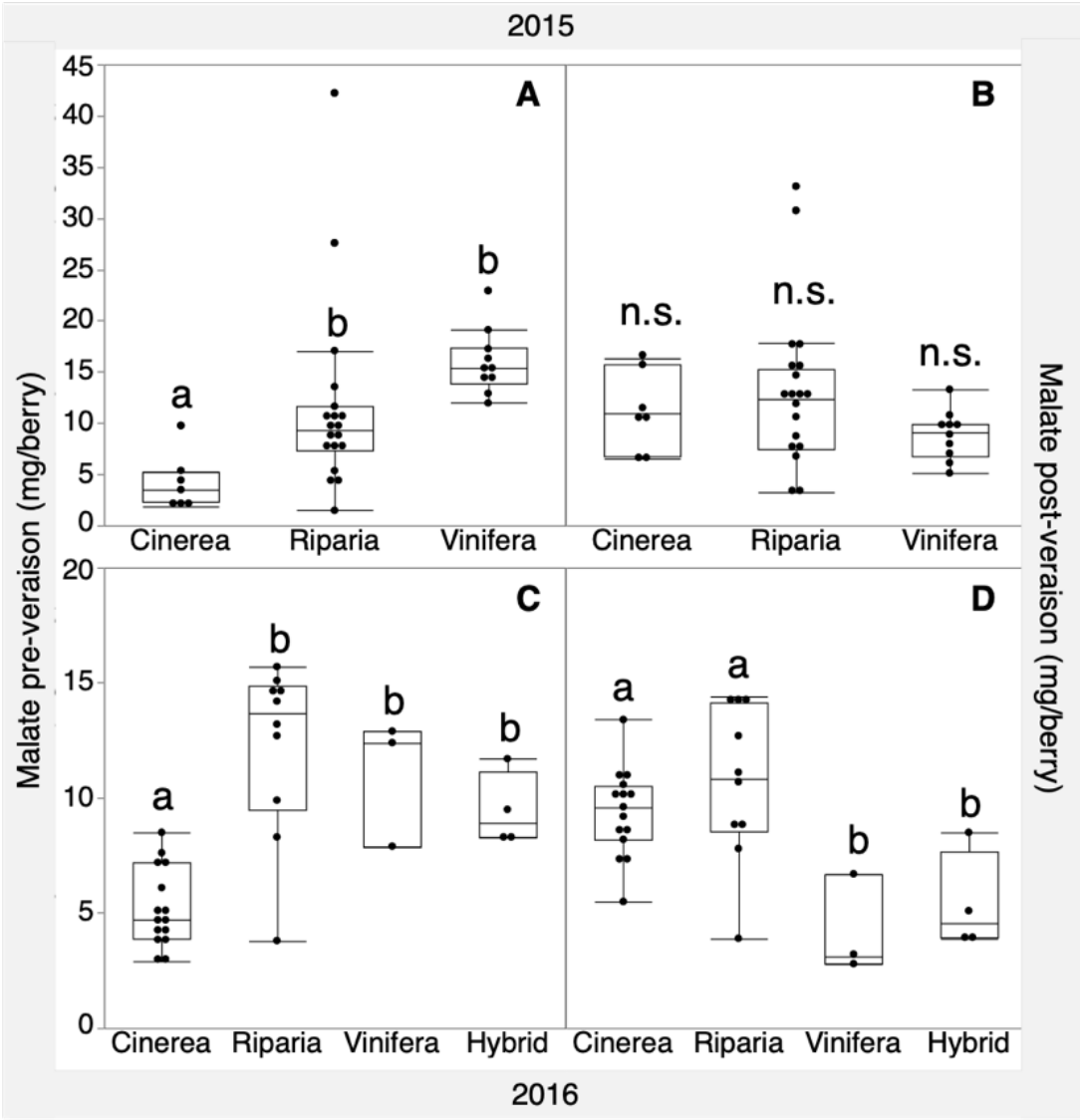

Figure 3.2: Box plots of malate content (mg/berry) by species, partitioned by both year and developmental time point (pre vs. post-veraison). A) Malate content by species for 2015 at -15 dpv ("pre-veraison"). B) Malate content by species for 2015 at 15 dpv ("post-veraison"). C) Malate content by species for 2016 at -11 dpv ("pre-veraison"). D) Malate content by species for 2016 at 19 dpv ("post-veraison"). Statistical analysis was performed using ln-transformed malate values for normalization; letters denote statistically different malate content ($p < 0.05$).

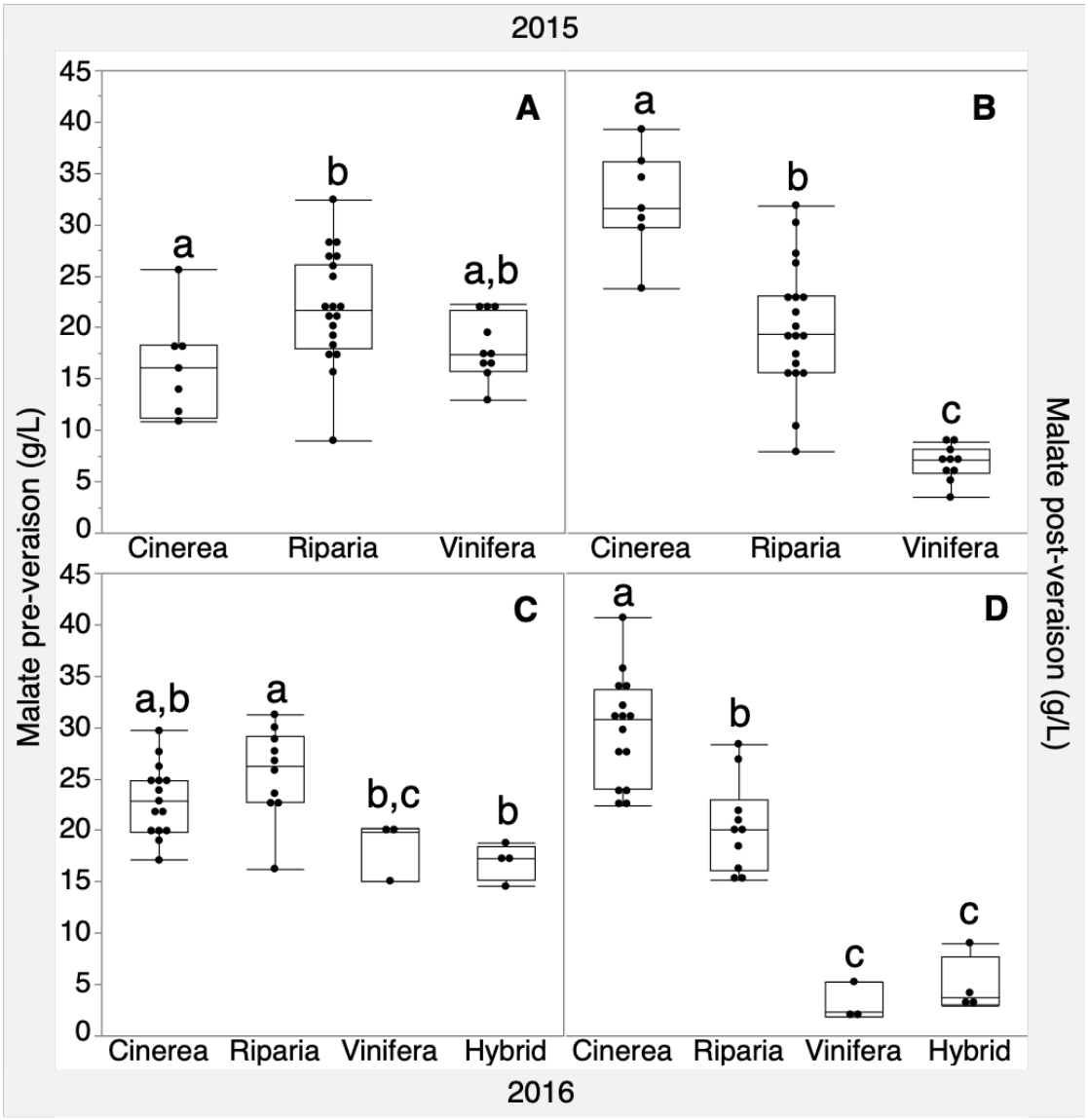

Figure 3.3: Box plots of malate concentrations (g/L) by species, separate by year and developmental time point (pre vs. post-veraison). A) Malate concentrations by species for 2015 at -15 dpv ("pre-veraison"). B) Malate concentrations by species for 2015 at 15 dpv ("post-veraison"). C) Malate concentrations by species for 2016 at -11 dpv ("pre-veraison"). D) Malate concentrations by species for 2016 at 19 dpv ("post-veraison"). Statistical analysis was performed using ln-transformed malate values for normalization; letters denote statistically different malate concentrations ($p < 0.05$).

Malate content for *V. vinifera* was consistent with literature values at both pre and post-veraison stages (Ruffner 1982; Kliewer et al. 1967). This is the first report of pre-veraison malate for *V. cinerea*, *V. riparia* and the interspecific hybrid cultivars. Post-

veraison values for *V. cinerea* and *V. riparia* (11.4 and 10.6 mg/berry for 2015; 10.0 and 9.2 mg/berry for 2016) were comparable to pre-veraison maximum of *V. vinifera*, and concentrations on a w/v basis (mean = 3.0 g malate/100 mL *V. cinerea* and 1.9 g malate/100 mL *V. riparia*) agree with a survey of organic acids in the fruit of mature *Vitis* spp. (Kliewer 1967). Malate per berry did not differ significantly between interspecific hybrids and *V. vinifera* cultivars, although this may be a consequence of the small number of samples used, as reanalysis of data in a previous survey (Haggerty 2013) did show significantly higher malate in hybrids on a concentration basis.

A further analysis compared the ratio of post-veraison malate content (mg / berry) to pre-veraison content (mg / berry). All three species differed significantly from each other in 2015 (Fig 4a). For 2016, the ratio followed the order *cinerea* > *riparia* > hybrid and *vinifera* for 2016 ($p<0.05$) (Figure 4b). For both years, malate content in *V. cinerea* increase by > 100% from pre-to-post veraison, while it remained nearly unchanged in *V. riparia*. In *V. vinifera*, malate decreased by ~50% in 2015 and 80% in 2016, and interspecific hybrids decreased by approximately 50%.

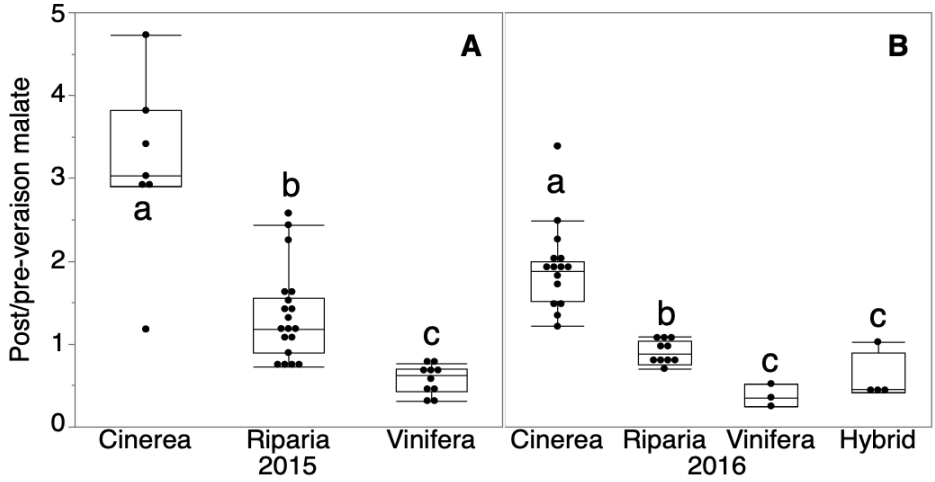

Figure 3.4: Box plots of the post/pre-veraison ratio of malate content (mg/berry) by species for 2015 (A) and 2016 (B). For 2015, "post/pre-veraison" are 15/-15 dpv respectively, and for 2016, they are 19/-11 dpv. Statistical analysis was performed using ln-transformed malate values for normalization; letters denote statistically different malate content ($p < 0.05$).

Across-year analysis indicates strong species-dependent malate behavior

Twelve of the wild *Vitis* accessions (six *V. cinerea* and six *V. riparia*) were measured in both 2015 and 2016, and regression of malate content across the two years is plotted in Figure 5. An ANOVA was performed to evaluate the effects of year, species, year-by-species, and accession on malate content. Results show that the dominant effect is species ($p < 0.001$), with a lesser effect of year ($p < 0.05$). Year-by-species and accession effects were both non-significant. The unexplained variation in pre-to-post veraison malate ratios within a species between the two years may indicate the presence of an accession-by-environment interaction. Malate degradation and to a lesser extent accumulation in *vinifera* are temperature dependent (Keller 2015), and speculatively these differences could be attributed to accession-dependent responses to the warmer 2016 season (2850 GDD) as compared to the 2015 season (2650 GDD) (Gerling and Walter-Peterson 2016).

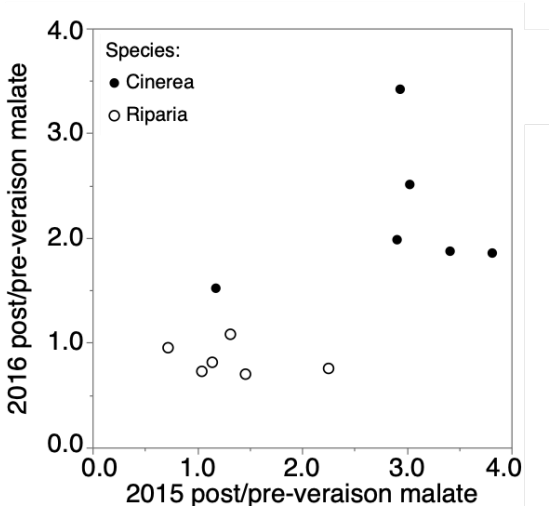

Figure 3.5: Post/pre-veraison ratios of malate content (mg/berry) for accessions of *V. cinerea* (n = 6) and *V. riparia* (n = 6) in 2015 and 2016. Each point represents the same accession, measured over two consecutive years.

Interspecific differences in grape malate behavior is led by the mesocarp

Previous work on *vinifera* reported that malate degradation during ripening is localized to the mesocarp, and that malate may increase slightly (~25%) in skins during berry maturation (Iland and Coombe 1988). To determine if variation in malate degradation among *Vitis* spp. could be related to variation in skin-to-mesocarp ratio, berries from *vinifera, cinerea* and *riparia* (two cultivars/accessions of each) were harvested at veraison and 30 days post-veraison and dissected. The proportion of skin tissue in *cinerea* and *riparia* berries reached 16 and 12% of berry mass respectively compared to 8% in *vinifera* berries (Supp. Table 2), with the last value agreeing with previous measurements of *V. vinifera* cv. Shiraz (Iland and Coombe 1988). The proportion of mesocarp was slightly higher in *vinifera* than in wild *Vitis* (87.5% vs. 73.4%, Supp. Table 2). More notable differences were observed in mesocarp malate content during ripening of *Vitis* spp. (Fig. 6a). In *vinifera*, malate in the mesocarp

decreased markedly (-80%) between veraison and 30 days post-veraison (loss of ~13 mg of malate per berry), comparable to results in Iland and Coombe (1988). In contrast, the change in mesocarp malate in wild *Vitis* spp. ranged from -24% to 13% in the 30 day period after veraison, with an average change of -10% (Fig. 6b). The difference between the average post-veraison change in mesocarp malate for wild *Vitis* spp. and *vinifera* (-10% vs. -80%) is comparable to difference in malate change observed in whole berries. Therefore, a likely explanation for the post-veraison variation in malate behavior among *Vitis* spp. is differences in mesocarp malate degradation, as opposed to differences in skin-to-mesocarp ratio.

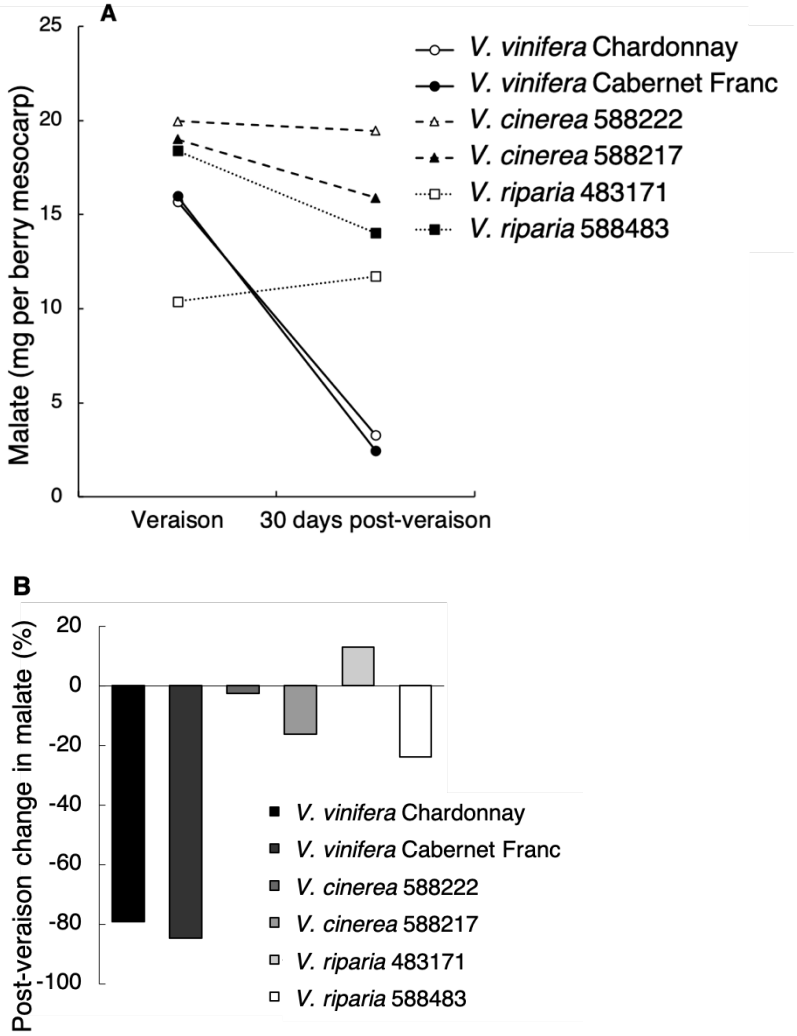

Figure 3.6: Malate in dissected fruit mesocarp tissues of three *Vitis* spp.: *vinifera, riparia,* and *cinerea*. Berries were sampled at the onset of veraison in each genotype, and 32-35 days later, during the 2018 growing season. A) Malate content per berry mesocarp at both ripening stages. B) Percent change in malate per berry in mesocarp in post-veraison fruit relative to its content at veraison.

Molecular and ecological explanations for differential malate behavior among Vitis species

A mechanistic explanation for differences in malate accumulation and degradation among *Vitis* spp. is not clear at this point. A molecular understanding for these differences would be of interest to grape breeders interested in low-malate phenotypes, and could also serve as a model for other fleshy fruits that show a range of organic acid behaviors during ripening, as discussed below. Although the enzymes directly involved in malate metabolism in *V. vinifera* and other fleshy fruits have been well-characterized, explanations for variation in fruit malate content – among genotypes, during maturation, or in response to environment – are lacking. Studies have attempted to correlate differences to key enzymes involved in malate metabolism, e,g. malate enzyme (NAD-ME) and PEPCK, however, the relation between expression or activity of these genes and malate behavior in grapes has been inconclusive (Sweetman et al. 2009). More recent work on organic acid accumulation in fleshy fruits has focused on the importance of vacuolar membrane transport. Malate (as an ionized dicarboxylate at cytosolic pH) is proposed to undergo facilitated diffusion through the tonoplast, before being protonated and trapped at vacuolar pH (Martinoia 2018). In apples, a major QTL (Ma1) associated with an aluminum activated malate transporter (ALMT) explained differences in acidity between low- and high-acid phenotypes (Bai et al. 2012). A functional homolog (VvALMT9) has been detected in *V. vinifera* (de Angeli et al. 2013), and a minor QTL for malate concentration in an ALMT-containing region has been reported in a *Vitis* spp. mapping population (Yang et al. 2016). The loss of malate in post-veraison *vinifera* is proposed to be related to

increasing vacuolar pH during ripening, which allows for diffusion of malate back into the cytosol (Terrier et al. 2001). Speculatively, the apparent continuation of malate accumulation in some wild accessions in our work could relate to differences in the timing of the expression of ALMT and other membrane transporters (e.g. proton pumps responsible for the acidification of the vacuole (Terrier et al. 2001)). The high rate of malate degradation in *vinifera* as compared to the other species could then relate to differences in tonoplast integrity post-veraison, or to differences in proton pump activity.

Our results also raise questions regarding the evolutionary role of malate degradation in post-veraison grapes. For example, the loss of malate during ripening is proposed to make grapes more attractive to frugivores (Keller 2015), which would be birds for small, dark-colored berries (e.g. *riparia*, *vinifera*, and *cinerea*). However, field experiments with artificial grapes have shown that although birds do prefer grapes with higher sugar content, bird feeding preferences are unrelated to acidity (Saxton et al. 2009). Furthermore, the behavior of acids in these wild *Vitis* is not unique among fleshy fruits. There are several fruits which show an increase in the concentration of their major organic acid or titratable acidity (or both) in maturing fruits, including strawberries (Moing et al. 2001) and kiwifruit (Walton and Jong 1990). In summary, it is evident that a loss of acidity during ripening is not a pre-requisite for *Vitis* spp. to attract frugivores.

A second hypothesis for why *vinifera* degrade malate post-veraison is that the berry shifts to using malate as a metabolic substrate so that it can accumulate sugars (Keller 2015). This hypothesis was proposed based on the observation that the

respiratory quotient (that is, the ratio of CO_2 produced to O_2 consumed) increases during veraison, suggesting that malate replaces hexoses as a substrate. However, a recent report calculated that malate respiration could account for only 20-30% of CO_2 production during ripening (Famiani et al. 2014), and that malate consumption would decrease sugar respiration by only 2% (or, approximately 0.4 Brix, assuming 20 Brix fruit). Interestingly, a survey of 21 Spanish accessions of *V. vinifera* L. ssp. *sylvestris* (the wild ancestor of domesticated *vinifera*) over 3 years reported acid concentrations more comparable to *V. riparia* and *cinerea* than to domesticated *vinifera* (Revilla et al. 2010). For example, in the 2008 growing season (the most extensively sampled) all *sylvestris* accessions had soluble solids associated with maturity in domesticated *vinifera* (> 20 Brix) but very high titratable acidity (range = 7.9-37.5 g/L, median = 15.3 g/L, presumably as tartaric acid equivalents). A potential explanation for the high titratable acidity in most *V. vinifera* L. ssp. *sylvestris* is that they have minimal malate degradation post-veraison, and that the malate-degrading (and, thus lower acid) phenotype associated with modern *V. vinifera* cultivars was selected during their domestication, as occurred for apples (*Malus*) (Khan et al. 2014). In this case, the evolutionary role of post-veraison malate degradation in domesticated *vinifera* was to satisfy the gustatory demands of humans, a pattern that continues with modern *Vitis* breeding efforts.

Conclusion

As compared to *vinifera*, wild *Vitis* spp. show reduced post-veraison degradation and in some cases post-veraison accumulation of malate on a per berry basis. These

differences appear to be related to changes in metabolism within the mesocarp as opposed to differences in skin to mesocarp ratios. Future studies on differences in malate behavior in *Vitis* spp., e.g. for QTL analyses of mapping populations, should account for the variability of the dynamic nature of this trait within the *Vitis* genus by including both pre- and post-veraison sampling points.

REFERENCES

de Angeli A, Baetz U, Francisco R, Zhang J, Chaves MM, Regalado A. 2013. The vacuolar channel VvALMT9 mediates malate and tartrate accumulation in berries of Vitis vinifera. Planta. 238(2):283–291.

Bai Y, Dougherty L, Li M, Fazio G, Cheng L, Xu K. 2012. A natural mutation-led truncation in one of the two aluminum-activated malate transporter-like genes at the Ma locus is associated with low fruit acidity in apple. Mol Genet Genomics. 287(8):663–678.

Chen J, Wang N, Fang LC, Liang ZC, Li SH, Wu BH. 2015. Construction of a high-density genetic map and QTLs mapping for sugars and acids in grape berries. BMC Plant Biol. 15(1):1–14.

Coquard Lenerz CTM. 2012. Phenolic extraction from red hybrid winegrapes. Cornell University.

Famiani F, Farinelli D, Palliotti A, Moscatello S, Battistelli A, Walker RP. 2014. Is stored malate the quantitatively most important substrate utilised by respiration and ethanolic fermentation in grape berry pericarp during ripening? Plant Physiol Biochem. 76:52–57.

Fresnedo-Ramírez J, Yang S, Sun Q, Cote LM, Schweitzer PA, Reisch BI, Ledbetter CA, Luby JJ, Clark MD, Londo JP, et al. 2017. An integrative AmpSeq platform for highly multiplexed marker-assisted pyramiding of grapevine powdery mildew resistance loci. Mol Breed. 37(145):1-16.

Gerling C, Walter-Peterson H. 2016. Veraison to Harvest #9. Accessed Dec 01, 2018. https://grapesandwine.cals.cornell.edu/sites/grapesandwine.cals.cornell.edu/files/shared/Veraison-To-Harvest-2016-Issue-9.pdf.

Haggerty LL. 2013. Ripening profile of grape berry acids and sugars in university of Minnesota wine grape cultivars, select Vitis vinifera, and other hybrid cultivars. University of Minnesota.

Iland PG, Coombe BG. 1988. Malate , Tartrate , Potassium , and Sodium in Flesh and Skin of Shiraz Grapes During Ripening : Concentration and Compartmentation. Am J Enol Vitic. 39(1):71–76.

Keller M. 2015. The Science of Grapevines: Anatomy and Physiology. 2nd ed. Waltham: Academic Press.

Khan MA, Olsen KM, Sovero V, Kushad MM, Korban SS. 2014. Fruit Quality Traits Have Played Critical Roles in Domestication of the Apple. Plant Genome. 7(3):1-18.
Kliewer W. 1967. Concentration of Tartrates, Malates, Glucose and Fructose in the Fruits of the Genus Vitis. Am J Enol Vitic. 18(2):87–96.
Kliewer WM, Howarth L, Omori M. 1967. Concentrations of tartaric acid and malic acids and their salts in Vitis Vinifera grapes. Am J Enol Vitic. 18(1):42–54.
Londo JP, Kovaleski AP. 2017. Characterization of wild North American grapevine cold hardiness using differential thermal analysis. Am J Enol Vitic. 68(2):203–212.
Martinoia E. 2018. Vacuolar transporters - Companions on a longtime journey. Plant Physiol. 176:1384-1407.
Moing A, Renaud C, Gaudillere M, Raymond P, Roudeillac P, Denoyes-Rothan B. 2001. Biochemical changes during fruit development of four strawberry cultivars. J Am Soc Hortic Sci. 126(4):394–403.
Plane R, Mattick L, Weirs L. 1980. An Acidity Index for the Taste of Wines. Am J Enol Vitic. 31(3):265–268.
Reisch BI, Owens CL, Cousins PS. 2012. Fruit breeding. In: Badenes ML, Byrne DH, editors. Fruit Breeding. New York. p. 225–262.
Revilla E, Carrasco D, Benito A, Arroyo-García R. 2010. Anthocyanin composition of several wild grape accessions. Am J Enol Vitic. 61(4):536–543.
Rice AC. 1974. Chemistry of Winemaking from Native American Grape Cultivars. In: Chemistry of Winemaking. Vol. 137. p. 88–115.
Ruffner HP. 1982. Metabolism of Tartaric and Malic Acids in Vitis: A Review-Part B. Vitis. 21:346–358.
Saxton VP, Creasy GL, Paterson AM, Trought MCT. 2009. Behavioral responses of european blackbirds and australasian silvereyes to varying acid and sugar levels in artificial grapes. Am J Enol Vitic. 60(1):82–86.
Sun Q, Gates MJ, Lavin EH, Acree TE, Sacks GL. 2011. Comparison of odor-active compounds in grapes and wines from vitis vinifera and non-foxy American grape species. J Agric Food Chem. 59(19):10657–10664.
Sweetman C, Deluc LG, Cramer GR, Ford CM, Soole KL. 2009. Regulation of malate metabolism in grape berry and other developing fruits. Phytochemistry. 70(11–12):1329–1344.
Terrier N, Sauvage FX, Ageorges A, Romieu C. 2001. Changes in acidity and in proton transport at the tonoplast of grape berries during development. Planta. 213(1):20–28.
Walton EF, Jong TM de. 1990. Growth and compositional changes in kiwifruit berries from three Californian locations. Ann Bot. 66(3):285–298.
Waterhouse AL, Sacks GL, Jeffery DW. 2016. Acids. In: Understanding Wine Chemistry. Chichester: Wiley & Sons, Ltd. p. 19–33.
Yang S, Fresnedo-Ramírez J, Sun Q, Manns DC, Sacks GL, Mansfield AK, Luby JJ, Londo JP, Reisch BI, Cadle-Davidson LE, et al. 2016. Next generation mapping of enological traits in an F2 interspecific grapevine hybrid family. PLoS One. 11(3):1–19.
Zoecklein BW, Fugelsang KC, Gump BH, Nury FS. 1999. Wine Analysis and Production. New York: Springer Science+Business Media.

CHAPTER 4

ADAPTING FOOD CHEMISTRY CONCEPTS TO THE HIGH SCHOOL CURRICULUM

ABSTRACT

As a means to ameliorate safety and environmental concerns with current curriculum, as well as expose students to the growing food systems industry, there is a need for more food science-related exercises in primary and secondary education. Specifically, we sought to develop a safe, high school appropriate, and demonstration-rich lesson plan based on aroma and flavor chemistry that is aligned with the Next Generation Science Standards (NGSS). To achieve this, we designed a set of experiments in which students observe and explain sensory changes that occur following physiochemical changes (e.g. pH shifts, heating) of commercially available flavoring materials (e.g. vanilla extract and essential oils) or foodstuffs. These experiments cover NGSS concepts including chemical reactions, equilibrium, and constructions of evidence-based theories based on observed phenomena, as well as introducing food science concepts in sensory evaluation and food chemistry. Evaluations will be performed using the NGSS "Educators Evaluating the Quality of Instructional Products (EQuIP)" rubric. Successful plans will be shared with other educators through outlets such as Chemical Solution, ChemMatters, and ChemEdX.

INTRODUCTION

There have been several incidents in recent years in high school chemistry classes which resulted in fatalities or severe injuries [1,2]. This has led to a re-evaluation of classroom safety [3], and an interest in identifying safe, instructive laboratory exercises that align with Next Generation Science Standards (NGSS) [4]. Concurrently, an increased need for food scientists [5] has resulted in attempts to increase awareness of food science at the primary, secondary, and post-secondary (undergraduate) education levels [6–8]. These efforts have been received positively by both students and instructors [9]. Prior work suggests that a food science-based scientific curriculum attracting students to STEM fields [10], and furthermore, recent findings indicate that incorporating food science modules into STEM education is a useful tool for teaching multidisciplinary science courses [11]. Science courses taught through food are reportedly more approachable, useful, relevant, easier to retain, and fun [10,12–14]. In addition to these benefits, materials for food science activities are typically easier to obtain and cheaper than traditional chemical reagents, as well as being more environmentally friendly and easier to dispose [9]. For example, all of our reagents for the activities described below were purchased from a local grocery store or online for ~$50.

Despite this, other than short modules on nutrition or food safety [15], there are few educational materials on food science designed for secondary school chemistry labs, and none relevant to flavor. A common demonstration is pigment separation to demonstrate chromatography [16,17]. Fischer esterification is also widely used in

post-secondary labs for teaching introductory concepts in synthesis [18,19], although its relevance to producing flavor compounds is often ignored.

This absence of materials for secondary school chemistry teachers related to aroma is striking because the chemistry of odorants (and odorant-matrix interactions) provides a rich environment for demonstrating core chemistry concepts. We sought to create activities similar to the one described in Kraft and Mannschreck [20], in which a core chemistry concept, e.g. stereochemistry, is taught using modalities, e.g. differences in familiar scents, that are interactive, safe, and touch upon basic principles of flavor chemistry, e.g. odor activity values.

GENERAL NOTES FOR INSTRUCTORS

These activities could be incorporated into learning modules regarding flavor, sensory perception, statistical analysis, classes of chemical structures, and analytical instrumentation. Activities 1 and 2 can be prepared ahead of time and presented via an instructor-only demonstration, or any/all of the activities can be performed as student experiments. The activities are easily divided into a station-style set-up with 2-3 students per group.

ACTIVITY 1: THE EFFECT OF PH CHANGES ON THE AROMA OF ACIDIC AND BASIC ODORANTS

Materials: Instant coffee, liquid aminos (unfermented liquid amino acids, e.g. Bragg Liquid Aminos), citric acid, pickling lime (CaOH), pH strips, water.

Expected learning outcomes: At the completion of the activity, students will be able to (1) Define the terms odorant, volatile, and aroma, 2) describe how changes in pH affected the aroma of coffee and aminos, and 3) describe how the charge of a compound can affect its volatility, and relate this to changes in the aroma of the two samples.

Activity overview: Students will label four jars as A (aminos at low pH), B (aminos at high pH), C (coffee at low pH), and D (coffee at high pH). Students will add 5 mL liquid aminos and 45 mL water to jars A and B, and the instant coffee (1/2 tsp in 50 mL hot water – per package instructions) to jars C and D. The students will then add citric acid (4 g) to 1 jar of liquid aminos and 1 jar of instant coffee. They will repeat this procedure using pickling lime (CaOH) (2 g) for the remaining 2 jars. The jars should be sealed, swirled, and sniffed. Odor observations should be recorded. After this, using a glass pipet, students should transfer 1 drop of each solution to a pH strip to determine final pH for each jar.

Discussion points: This activity works with any aroma compound that acts as an acid or base (i.e. primary odorants in coffee and liquid aminos are carboxylic acids). Students could calculate pK_a as a post-activity exercise. Like other demonstrations in the literature [21,22], this activity is using the human nose as a pH probe, and

therefore could be a useful adaptation for teaching pH changes to visually impaired students instead of colorimetric tests [23].

Figure 4.1: Liquid aminos and instant coffee at low and high pH.

ACTIVITY 2: THE EFFECT OF TEMPERATURE ON AROMA

Materials: cherry and green apple extracts, hot plate, ice bath

Expected learning outcomes: At the completion of the activity, students will be able to discuss how (1) temperature affects the concentration and type of flavor used in food products; (2) "fruity" smelling compounds (esters) degrade at high temperature.

Activity overview: Students will prepare 6 beakers, each containing 50 mL of water. Beakers (2) should be placed on a hot plate. The water should be allowed to warm to ~ 33°C. Beakers (2) should be placed in an ice bath and allowed to chill to ~ 0°C. Beakers (2) should sit at room temperature. When designated temperatures have been reached, students should add 3 drops of the cherry extract to one set of beakers, and 3 drops of green apple extract to the other set of beakers. The beakers should be sealed with parafilm, allowed to rest for 1 minute, then swirled and sniffed. Observations should be recorded.

Figure 4.2: Demonstration of the effects of temperature on aroma.

Discussion points: The cherry and green apple extracts are conducive to the discussion of thermal degradation and ethyl ester hydrolysis, because they are rich in these volatile esters. The cherry extract would contain isobutyl acetate, and other generally fruity esters; the green apple extract would predominantly be ethyl hexanoate and hexyl acetate, i.e. the key odorants responsible for that aroma [24]. Furthermore, this activity could be used as an introduction to more advanced thermodynamic principles, such as the Clausius-Clapeyron relationship and Henry's Law.

For example, if the vapor pressure of ethyl hexanoate is 0.108 atm at 98.98 °C (372.13 K), and the enthalpy of vaporization is 49.5 kJ/mol [25], we can estimate the vapor pressure at 33°C (306.15 K) using the Clausius-Clapeyron equation:

$$ln\left(\frac{P_1}{P_2}\right) = -\frac{\Delta H_{vap}}{R}\left(\frac{1}{T_1} - \frac{1}{T_2}\right)$$

Rearranged to:

$$P_1 = e^{\wedge}\left[-\frac{\Delta H_{vap}}{R}\left(\frac{1}{T_1}-\frac{1}{T_2}\right)\right] \times P_2$$

Which gives us:

$$P_{33} = e^{\wedge}\left[-\left(\frac{49{,}500\ J/mol}{8.3145\ J/mol \times K}\right)\left(\frac{1}{306.15\ \text{K}}-\frac{1}{372.13\ \text{K}}\right)\right] \times 0.108\ \text{atm} = 0.69\ \text{atm}$$

ACTIVITY 3: FLAVOR: TASTE, SMELL AND CHEMESTHESIS INTERACTIONS

Materials: vanilla extract, salt, sugar, citric acid, paper cups, nose clips, peppermint extract

Expected learning outcomes: At the completion of the activity, students will be able to describe (1) how additives affect flavor release from food, (2) how additives/sensory deprivation affect flavor recognition, (3) be able to define chemesthesis.

Activity overview: Students should each fill 5 paper cups as listed below:

Table 4.1: Preparation instructions for Activity 3

CUP #:	Water to add (mL):	Food matrix addition:	Flavorant addition:
1	50	Salt: 0.75 g	Vanilla: 5 drops
2	50	Sugar: 2 g	Vanilla: 5 drops
3	50	Citric acid: ~0.25 g (pH 3)	Vanilla: 5 drops
4	50	N/A	Peppermint: 15 drops
5	50	N/A	Vanilla: 10 drops

For all cups, the solution should be swirled, sipped, and expectorated into an extra paper cup, and observations recorded. Before tasting cups 4 and 5, the students should put on nose clips. After experiencing the taste *with* nose clips, the students should remove the nose clips, and re-taste.

Figure 4.3: Demonstration of chemesthesis effect and masking effect using peppermint and vanilla extracts, and nose clips.

Discussion points: For cup 3, alternatively, the instructor could prepare the citric acid solution prior to class. Different flavor extracts or additives (artificial sugars, starch, protein, other preservatives, e.g. ascorbic acid) could be used in this demonstration. It could also be applied to examine the effects of fat content: e.g. 10 drops of vanilla in 50 mL neutral oil, or milk of varying milk fat percentages. This activity is applicable to the learning of equilibrium constants and to the decoupling the broader concept of "flavor" into its three components (senses): taste, smell, and chemesthesis (i.e. chemically induced tactile sensations) [26]. The activity could also be utilized in a biology or biochemistry class, as it leads well into a discussion of taste

bud anatomy and types of receptors (e.g. GPCRs, ion channels). A prior study found that since baseline knowledge of food science is negligible in secondary education, activities can be incorporated into either biology or chemistry courses with no significant difference in students' ability to comprehend basic food science principles [27].

DISCUSSION

The Next Generation Science Standards were developed with input from 26 states, as well as the National Research Council, the National Science Teachers Association, the American Association for the Advancement of Science, and Achieve, Inc. [4]. New York State was a Lead State Partner in the development phase, and has based its recently revised science curriculum, NYSP-12SLS, on the NGSS [28]. The NGSS are built on a three-dimensional framework for science learning: "the *practices* through which scientists and engineers do their work; the key *crosscutting concepts* that link the science disciplines; and the *core ideas* of the disciplines of life sciences, physical sciences, earth and space sciences, and engineering and technology" [29]. These three dimensions are consistent across primary and secondary education, and are incorporated into performance expectations (PEs), which are specific objectives for each grade level. Therefore, there is a learning progression throughout students' education in which they build upon a foundation of consistent themes with increasing sophistication and complexity [29]. Due to the rigorous body of research that was referenced in the design of NGSS, and the incorporation of NGSS by New York State,

we developed our flavor chemistry module to be compatible with NGSS, as detailed below.

To facilitate implementation of our module into an outreach initiative, we converted activity 1 (the effect of pH on the aroma of acidic and basic odorants) into a formalized lesson plan, in accordance with the American Association of Chemistry Teachers standards (see appendix). The lesson plan is comprised of a section for the teacher, as well as the student handout. The "For the Teacher" section includes a summary of scope of activity, objectives, chemistry topics that the lab demonstrates, and learning objectives supported via the activity. For activity 1, the following NGSS learning objectives are supported: Performance Expectation (PE) HS-PS3-6 ("…design of a chemical system by specifying a change in conditions…"), Science and Engineering Solutions Constructing Explanations and Designing Solutions, Disciplinary Core Ideas PS1-B Chemical Reactions, and ETS1.C Optimizing the Design Solution, and Crosscutting Concept Stability and Change. These are supported because the students change a chemical system (i.e. adjust pH) in several solutions and observe how that affects sensory perception. This segues into discussions and demonstrations regarding other perturbations to a chemical system that could lead to sensory perception changes, e.g. temperature (activity 2), matrix components (activity 3), as well as how perturbations to our own sensory system can inhibit or alter perception (activity 3). A summary of NGSS learning objectives supported through all 3 activities is summarized in table 4.2 below:

Table 4.2: Summary of NGSS that are demonstrated through each activity. PE = performance expectation, HS = high school (grades 9-12), PS = physical sciences discipline, LS = life sciences discipline, DCI = disciplinary core idea, ETS = Engineering, Technology, and Applications of Science. The topic for PS1 is Matter and Interactions; the topic for LS1 is From Molecules to Organisms: Structures to Processes.

Activity (right); NGSS (below):	1: Aroma as pH Indicator	2: Temperature & Aroma	3: Flavor: Taste, Smell, & Chemesthesis Interactions
PE HS-PS1-5	No	Yes	No
PE HS-PS1-6	Yes	Yes	Yes
PE HS-LS1-2	No	No	Yes
DCI PS1.B	Yes	Yes	Yes
DCI LS1.A	No	No	Yes
DCI ETS1.C	Yes	Yes	No
Sci & Eng Practices	Constructing Explanations	Constructing Explanations	Constructing Explanations Developing & Using Models
Crosscutting Concept	Stability & Change	Stability & Change/Patterns	Stability & Change Systems & System Models

In addition, as listed in the lesson plan learning objectives, activity 1 meets the AP Chemistry Curriculum Framework Big Idea 6, specifically 6.B ("systems at equilibrium are responsive to external perturbations, with the response leading to a change in the composition of the system") and 6.C ("chemical equilibrium plays an important role in acid-base chemistry and in solubility").

The "For the Teacher" section of the lesson plan also provides both prep and active demonstration time estimates, materials needed, safety instructions, and notes for the teacher. The Teacher Notes includes recommendations for students' baseline knowledge, facilitation of the activity, and suggestions for higher level differentiation of the activity (e.g. an honors or AP course). The "For the Student" section contains a brief introduction to aroma chemistry, and frames the lab's relevancy to understanding pH, acids and bases, and system perturbations. There are also prelab questions, materials needed, safety instructions, experimental procedure, charts for data entry,

post-lab analysis questions, and conclusions. The conclusions are thought questions asking students to reflect on the information provided, as well as their own observations, to hypothesize beyond the scope of the lab exercise itself.

In addition to questions related to the activity itself, we also seek to assess the effectiveness of knowledge transfer (cognitive domain) and student engagement (affective domain). This two evaluation matrices are common in both formal education environments and extension/outreach-based programming, and are supported by multiple learning theories, especially Novak's Theory of Meaningful Learning and Human Constructivism [30] and Bloom's taxonomy [31]. In measuring cognitive domain, we seek to understand how effective we were at teaching in a "traditional" sense: did the students comprehend the subject matter, e.g. can they now define flavor chemistry? And in evaluating affective domain, we gain valuable feedback on attitudes, motivation, and willingness to incorporate new values (knowledge) into a lifestyle, e.g. did the students find this lab activity intriguing? [31]. Therefore, we have designed a Student Knowledge, Attitudes, and Behaviors Assessment (see appendix). This assessment will be administered both pre- and post-lab during preliminary classroom implementation. It contains questions to assess students' understanding of flavor chemistry, and their interest in the subject matter [27,32,33]. The comparison of pre- to post-test scores will enable us to acquire insights into the impact of our module, and revise accordingly before communicating to a wider audience, e.g. the AACT classroom resources library.

REFERENCES

[1] J. Kemsley, Improving Chemistry Demonstration Safety, Chem. Eng. News. 92 (2014) 38.

[2] K. Roy, Safer Science: Better Practices for Safety Issues in the Science Classroom and Laboratory, Sci. Teach. (2016) 56.

[3] J. Kemsley, How To Make Chemistry Classroom Demonstrations And Experiments Safer, Chem. Eng. News. 93 (2015) 37–39.

[4] NGSS Lead States. 2013. *Next Generation Science Standards: For States, By States.* Washington, DC: The National Academies Press.

[5] C.D. Stevenson, Toward Determining Best Practices for Recruiting Future Leaders in Food Science and Technology, J. Food Sci. Educ. 15 (2016) 9–13. doi:10.1111/1541-4329.12078.

[6] B. Schaich-rogers, Schaich-Rogers (2007) Training teachers to use food to teach science_Journal of Food Science Education_2007, 6 (2007) 17–21.

[7] J.C. McEntire, M. Rollins, A Two-Pronged Approach to Promote Food Science in U.S. High Schools, J. Food Sci. Educ. 6 (2007) 7–13.

[8] A.M. Liceaga, T.S. Ballard, L.T. Esters, Increasing content knowledge and self-efficacy of high school educators through an online course in food science, J. Food Sci. Educ. 13 (2014) 28–32. doi:10.1111/1541-4329.12028.

[9] S.B. Mitchell, Experimenting with the Sweet Side of Chemistry: Connecting Students and Science through Food Chemistry, J. Chem. Educ. 91 (2014) 1509–1510. doi:10.1021/ed5007458.

[10] S.J. Schmidt, D.M. Bohn, A.J. Rasmussen, E.A. Sutherland, Using Food Science Demonstrations to Engage Students of All Ages in Science, Technology, Engineering, and Mathematics (STEM), J. Food Sci. Educ. 11 (2012) 16–22. doi:10.1111/j.1541-4329.2011.00138.x.

[11] J.A. Hovland, V.G. Carraway-Stage, A. Cela, C. Collins, S.R. Díaz, A. Collins, M.W. Duffrin, Food-based science curriculum increases 4th graders multidisciplinary science knowledge, J. Food Sci. Educ. 12 (2013) 81–86. doi:10.1111/1541-4329.12016.

[12] P. Bell, Design of a Food Chemistry-Themed Course for Nonscience Majors, J. Chem. Educ. 91 (2014) 1631–1636. doi:10.1021/ed4003404.

[13] B. Calder, S.H. Brawley, M. Bagley, National Science Foundation Graduate Teaching Fellows Promote Food Science Education in K-12 Schools in Maine, J. Food Sci. Educ. 2 (2003) 58–60.

[14] D.T. Miles, A.C. Borchardt, Laboratory Development and Lecture Renovation for a Science of Food and Cooking Course, J. Chem. Educ. 91 (2014) 1637–1642. doi:10.1021/ed5003256.

[15] T.K. Chapin, R.C. Pfuntner, M.J. Stasiewicz, M. Wiedmann, A. Orta-Ramirez, Development and Evaluation of Food Safety Modules for K-12 Science Education, J. Food Sci. Educ. 14 (2015) 48–53. doi:10.1111/1541-4329.12050.

[16] D.A. Forss, A chromatographic demonstration, J. Chem. Educ. 32 (1955) 306. doi:10.1021/ed032p306.

[17] G.W. Chism, Chromatography of Food Dyes: A Simple Demonstration for Actively Engaging High School Students in the Chemistry of Foods, J. Food Sci. Educ. 1 (2008) 18–23. doi:10.1111/j.1541-4329.2002.tb00006.x.
[18] P.A. Wade, S.A. Rutkowsky, D.B. King, A Simple Combinatorial Experiment Based on Fischer Esterification. An Experiment Suitable for the First-Semester Organic Chemistry Lab, J. Chem. Educ. 83 (2006) 927. doi:10.1021/ed076p1560.
[19] J. V. McCullagh, S.P. Hirakis, Synthesis of the Commercial Fragrance Compound Ethyl 6-Acetoxyhexanoate: A Multistep Ester Experiment for the Second- Year Organic Laboratory, J. Chem. Educ. 94 (2017) 1347−1351. doi:10.1021/acs.jchemed.6b00778.
[20] P. Kraft, A. Mannschreck, The enantioselectivity of odor sensation: Some examples for undergraduate chemistry courses, J. Chem. Educ. 87 (2010) 598–603. doi:10.1021/ed100128v.
[21] K. Neppel, M.T. Oliver-Hoyo, C. Queen, N. Reed, A Closer Look at Acid–Base Olfactory Titrations, J. Chem. Educ. 82 (2005) 607. doi:10.1021/ed082p607.
[22] J.T. Wood, R.M. Eddy, Olfactory Titration, J. Chem. Educ. 73 (1996) 257. doi:10.1021/ed073p257.
[23] M.N. Flair, W. N. Setzer, An Olfactory Indicator for Acid-Base Titrations, J. Chem. Educ. 67 (1990) 795-796. doi:10.1021/ed067p795.
[24] A.L. Waterhouse, G.L. Sacks, D.W. Jeffery, Understanding Wine Chemistry, Wiley, Chichester, 2016. doi:10.1002/9781118730720.
[25] M. Benziane, K. Khimeche, I. Mokbel, T. Sawaya, A. Dahmani, J. Jose, Experimental Vapor Pressures of Five Saturated Fatty Acid Ethyl Ester (FAEE) Components of Biodiesel, J. Chem. Eng. Data 56 (2011) 4736-4740. doi:10.1021/je200730m.
[26] H.T. Lawless, H. Heymann, Sensory Evaluation of Food, 2nd ed., Springer, New York, 2010. doi:10.1007/978-1-4419-6488-5.
[27] E.I. Stringer, J.D. Hendrix, K.A. Swortzel, J.B. Williams, M.W. Schilling, Evaluating the Effectiveness of Integrating Food Science Lessons in High School Biology Curriculum in Comparison to High School Chemistry Curriculum, J. Food Sci. Educ. 0 (2018) 1–8. doi:10.1111/1541-4329.121
[28] http://www.nysed.gov/common/nysed/files/programs/curriculum-instruction/nysscienceintro.pdf. Accessed 05.01.19
[29] National Research Council. (2014). *Developing Assessments for the Next Generation Science Standards.* Committee on Developing Assessments of Science Proficiency in K-12. Board on Testing and Assessment and Board on Science Education, J.W. Pellegrino, M.R. Wilson, J.A. Koenig, and A.S. Beatty, *Editors.* Division of Behavioral and Social Sciences and Education. Washington, DC: The National Academies Press.
[30] K.R. Galloway and S.L. Bretz, Development of an Assessment Tool to Measure Students' Meaningful Learning in the Undergraduate Chemistry Laboratory, J. Chem. Educ. 92 (2015) 1149-1158. doi:10.1021/ed500881y.
[31] R.W. Hartel and W.T. Iwaoka, A Report from the Higher Education Review Board (HERB): Assessment of Undergraduate Student Learning Outcomes in

Food Science, J. Food Sci. Educ. 15 (2016) 56–62. doi:10.1111/1541-4329.12084.
[32] J.R. Richards, G. Skolits, J. Burney, A. Pedigo, F.A. Draughon, Validation of an Interdisciplinary Food Safety Curriculum Targeted at Middle School Students and Correlated to State Educational Standards, J. Food Sci. Educ. 7 (2008) 54–61. doi:10.1111/1541-4329.2008.00051x.
[33] C.L. Wickware, C.T.C Day, M. Adams, A. Orta-Ramirez, A.B. Snyder, The Science of a Sundae: Using the Principle of Colligative Properties in Food Science Outreach Activities for Middle and High School Students, J. Food Sci. Educ. 16 (2017) 92–98. doi:10.1111/1541-4329.12112.

CHAPTER 5

CONCLUSIONS AND FUTURE DIRECTIONS

In chapter 2, we developed a methodology for assessing the amount of error (%RSD) introduced by using non-matched internal standards when quantitating volatiles using HS-SPME-GS-MS. These Compound × Individual matrix effects were found to result in %RSDs ranging from 17-249% in a grape (*Vitis* spp.) mapping population, and from 8-56% in a tomato (*Solanum* spp.) recombinant inbred line population. Furthermore, it was observed that the extent of these Compound × Individual matrix effects could not be estimated based on structural similarities between two compounds. The overall goal of this project, and potential future work, is to create a volatile screening methodology that maintains accurate quantitation, while accelerating the throughput, so that plant breeders can identify fruit quality QTLs.

Future directions of this work are to: 1) assess minimum sampling for identification of well-matched surrogate internal standards through Monte Carlo simulations, 2) to screen for novel volatile targets in the USDA-ARS grape germplasm and in VitisGen project populations using this surrogate standards approach, and 3) to validate the technique through standard additions or re-processing. For 1), prior data sets could be utilized to conduct Monte Carlo simulations. The purpose of the simulations is to ascertain the minimum number of samples necessary for identifying well-matched surrogate standards. The minimum sample size is found at the point when the %RSD of a Compound × Individual comparison is remaining constant, and a well-matched surrogate standard is defined as a surrogate within an acceptable %RSD.

Speculating on pitfalls, it is possible that the sample size to meet our desired parameters will be too high to accommodate fledgling breeding populations. It is also possible that we will be able to find well-matched surrogates for some compound classes, but will have difficulties with others.

For 2), wild *Vitis* spp. from the USDA-ARS germplasm, as well as grape populations from the VitisGen populations, could be processed using a cocktail of internal standards. In the post-hoc analysis, the samples could be screened for novel targets that contribute to the aroma of the final wine product, specifically those believed to have a positive correlation with wine quality. Volatiles will be quantitated using multiple internal standards from the cocktail, and the surrogate with the lowest %RSD tentatively identified as the most accurate. For 3), to validate accuracy, isotopically labeled isotopologues of the volatile target(s) could be purchased or synthesized. A subset of samples would then be re-processed, and the isotopically labeled standard utilized. An alternate strategy for validation of the quantitative capability of the surrogate standard would be to perform a standard addition study. For this method to be possible, the volatile target of interest would need to be commercially available. Both validation methods are time consuming [1], and we speculate that the success will depend on the robustness of the targeted novel analyte. For initial pursuit of this objective, an analyte that has previously been identified in a grape matrix at above sensory threshold would be ideal.

In chapter 3, we conducted a two-year study evaluating malic acid content across *Vitis* spp. Our findings indicate that, as compared to *vinifera*, wild *Vitis* spp. show

reduced post-veraison degradation and in some cases post-veraison accumulation of malate on a per berry basis. These differences appear to be related to changes in metabolism within the berry mesocarp as opposed to differences in skin to mesocarp ratios. Future work on this project has been proposed by Noam Reshef, PhD, a post-doctoral fellow in the Sacks lab. He will be investigating the molecular explanation behind the observed phenomena to identify stronger QTLs, or even candidate genes, related to malate utilization by the cell at key states of berry development.

Another potential future direction for this project would be surveying of malate in other *Vitis* species. Of particular interest would be a comparison of malate content across a growing season between the wild *Vitis* species, *aestivalis*, and the elite interspecific hybrid cultivar Norton. *V. aestivalis* is native to much of the eastern United States [2]. Norton is a hybrid believed to have been originally crossed in the early to mid-1800s [3]. Its parentage is estimated to be between 25-30% *vinifera* [4,5], with *aestivalis* as the predominant wild *Vitis* parent [3]. Norton is the official grape of the State of Missouri, and is widely planted throughout the southeastern and midwestern United States because of its resistance to fungal diseases (powdery mildew, downy mildew, various berry rots) and phylloxera, PD tolerance, and cold hardiness [4]. Like other interspecific hybrids, Norton suffers from organoleptic challenges, including high titratable acidity (8.5-13 g/L) and high pH (3.4-3.8), which are attributed to high malic acid in the fruit (~6 g/L at maturity) [6].

As discussed in chapter 3, there is a lack of understanding of malate content variation due to genetic differences, and the variation is compounded by well-reported environmental factors that lead to changes in malate, e.g decreased cluster shading and

increased temperature [7,8,9]. In our own work, we observed a decrease in malate content across species due the higher GDD in 2016 versus 2015. This indicates that at least a portion of malate content is regulated similarly across *Vitis* spp., though the question remains whether other malate reservoirs are shunted to different pathways in *V. vinifera* versus other *Vitis* spp., and where on the continuum the interspecific hybrids fall.

Therefore, we speculate that a study of *V. aestivalis* versus Norton would be advantageous for maximizing genetic similarity (many hybrids have much more complex parentages) and could lead to a more pronounced understanding on the effects of environment on malate content, i.e. what percent of variance in malate content can be attributed to environmental factors and an estimation of malate regulation conservation from a wild *Vitis* spp. to its hybrid offspring. Furthermore, a microsatellite-based genetic linkage map for Norton has recently been constructed, which could be a highly suitable reference genome for QTL analysis and candidate gene identification [4].

In chapter 4, we developed a flavor chemistry module appropriate for upper-level secondary education. The module contains 4 activities that demonstrate changes in compound volatility and aroma perception due to pH, temperature, and matrix, as well as an activity on decoupling the components of flavor, i.e. smell, taste, tactile sensations. The module is in alignment with the Next Generation Science Standards, and a pre- and post-module assessment measuring both knowledge transfer and student engagement has been created to evaluate programmatic success. The final

component of the project will be an implementation step, which will be conducted in conjunction with high school science educators in New York State.

REFERENCES

[1] P. Schieberle, R.J. Molyneux, Quantitation of Sensory-Active and Bioactive Constituents of Food: A Journal of Agricultural and Food Chemistry Perspective, J. Agric. Food Chem. 60:10 (2012), 2404–2408.

[2] S.T. Callen, L.L. Klein, A.J. Miller, Climatic Niche Characterization of 13 North American Vitis Species, Am. J. Enol. Vitic. 67:3 (2016) 339-349.

[3] B.I. Reisch, R.N. Goodman, M-H. Martens, N.F. Weeden, The Relationship Between Norton and Cynthiana, Red Wine Cultivars Derived from Vitis aestivalis, Am. J. Enol. Vitic. 44:4 (1993) 441-444.

[4] M. Hammers, S. Sapkota, L-L. Chen, CF. Hwang, Constructing a genetic linkage map of Vitis aestivalis-derived "Norton: and its use in comparing Norton and Cynthiana, Mol. Breeding 37:64 (2017) 1-14.

[5] Z. Migicovsky, J. Sawler, D. Money, R. Eibach, A.J. Miller, J.J. Luby, A.R. Jamieson, D. Velasco, S. von Kintzel, J. Warner, W. Wuhrer, P.J. Brown, S. Myles, Genomic ancestry estimation quantifies use of wild species in grape breeding, BMC Genomics 17:478 (2016) 1-8.

[6] G.L. Main, J.R. Morris, Leaf-Removal Effects on Cynthiana Yield, Juice Composition, and Wine Composition, Am. J. Enol. Vitic. 55:2 (2004) 147-152.

[7] Keller M. 2015. The Science of Grapevines: Anatomy and Physiology. 2nd ed. Waltham: Academic Press.

[8] I. Ryona, B.S. Pan, D.S. Intrigliolo, A.N. Lakso, G.L. Sacks, Effects of Cluster Light Exposure on 3-Isobutyl-2-methoxypyrazine Accumulation and Degradation Patterns in Red Wine Grapes (Vitis vinifera L. Cv. Cabernet Franc), J. Agric. Food Chem. 56:22 (2008), 10838–10846.

[9] T.K. Wolf, R.M. Pool, L.R. Mattick, Responses of Young Chardonnay Grapevines to Shoot Tipping, Ethephon, and Basal Leaf Removal, Am. J. Enol. Vitic. 37:4 (1986) 263-268.

APPENDIX

CHAPTER 2 SUPPLEMENTARY MATERIALS

MATERIALS & METHODS

Chemical Reagents and Standards for [U^{13}C]Hexanal and [U^{13}C]Hexanol Synthesis

The following chemicals were purchased from Sigma-Aldrich (St. Louis, MO): linoleic acid (95%), [U^{13}C] α-linoleic acid (>97%; >98% 13C enrichment), Soybean lipoxygenase (LOX) (EC No. 1.13.11.12) type I-B (221700 units/mg), alcohol dehydrogenase (ADH) from *Saccharomyces cerevisiae* (15000 units/mg), β-Nicotinamide adenine dinucleotide (NADH), reduced disodium salt hydrate (>94%), hexanal (≥97%), and hexanol (≥98%). Chemicals for buffers (citric acid (≥99%), sodium phosphate mono- (≥99%), and di-basic (≥98%), sodium bicarbonate (≥99%), and sodium carbonate (≥99%)) and organic solvents – ethanol (≥98%; EtOH), methanol (≥99%; MeOH), dichloromethane (≥99%; DCM), and pentane (≥99%) – were also purchased from Sigma Aldrich.

Preparation of Stock and Working Solutions for [U^{13}C]Hexanal and [U^{13}C]Hexanol Synthesis

<u>*Enzyme solutions:*</u> Separate solutions of LOX (753780 units/mL) and ADH (39300 units/mL stock solution were prepared by addition to 20 mL of Milli-Q water. Each stock was then stored in glass vials at -80 °C in 1.5 mL aliquots and thawed prior to use.

<u>*Chemical Standards:*</u> A solution of linoleic acid (5% w/w) was prepared by weighing 0.5 g of linoleic acid into 9.5 g of EtOH. [U^{13}C]linoleic acid stock solution (0.1 g was diluted in EtOH solution yielding a 5.95% w/w stock solution. Unlabeled hexanal and hexanol were prepared in EtOH to yield 10 and 100 µg/mL working solutions. NADH stock solution was prepared by adding 20 mL of Milli-Q water into 1 g of NADH yielding a stock concentration of 0.05 g/mL.

Buffer solutions: pH 4.5, pH 7.0, and pH 9.5 buffer solutions were prepared from 0.1 M citric acid/0.2 M sodium phosphate dibasic, 0.1 M sodium phosphate dibasic /0.1 M sodium phosphate monobasic, and 0.1 M sodium bicarbonate/0.1 M sodium carbonate respectively. The solutions were stored at 3 °C.

Protocol for Enzymatic Synthesis of [U^{13}C]hexanal and [U^{13}C]hexanol from [U-^{13}C]α-linoleic acid

The protocol for generating [U^{13}C]hexanal and [U^{13}C]hexanol is shown in Figure S.1. The yield of hexanal and hexanol was determined by calibration against unlabeled standards on GC-MS.

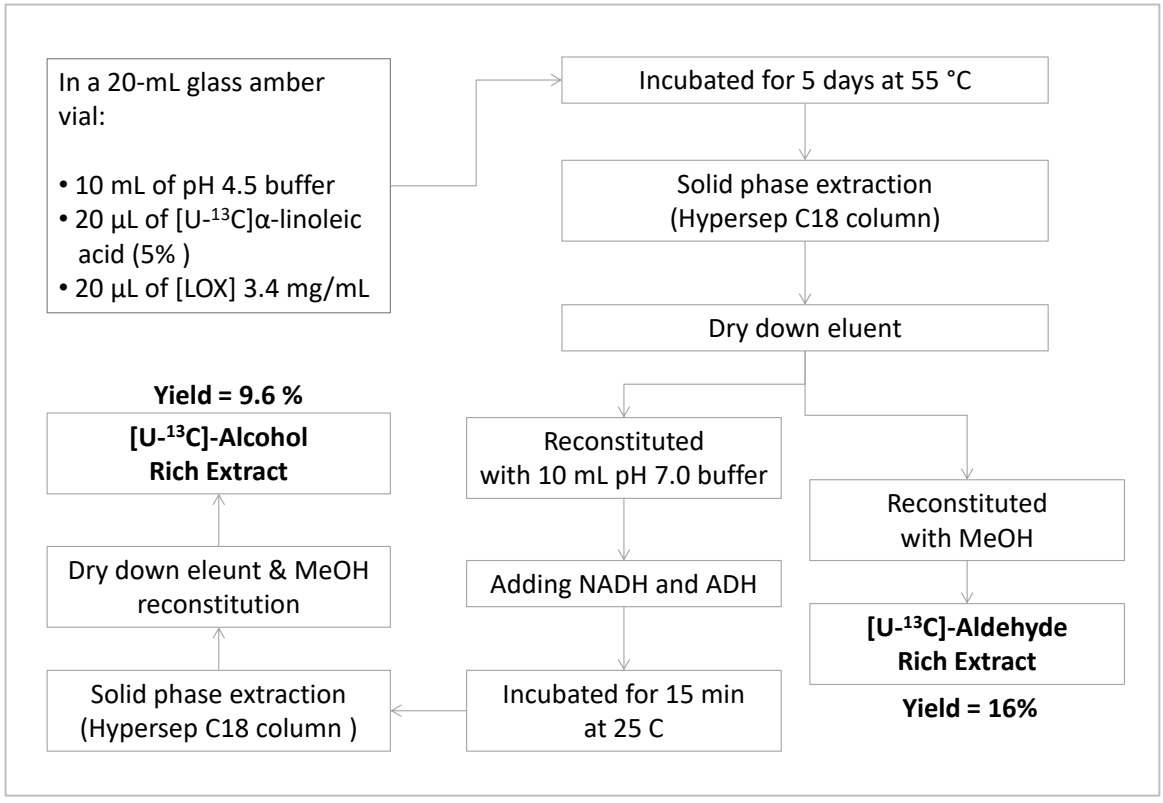

Figure S.1 – Protocol for generation of [U-^{13}C]hexanal and [U-^{13}C]hexanol from [U-^{13}C]α-linoleic acid.

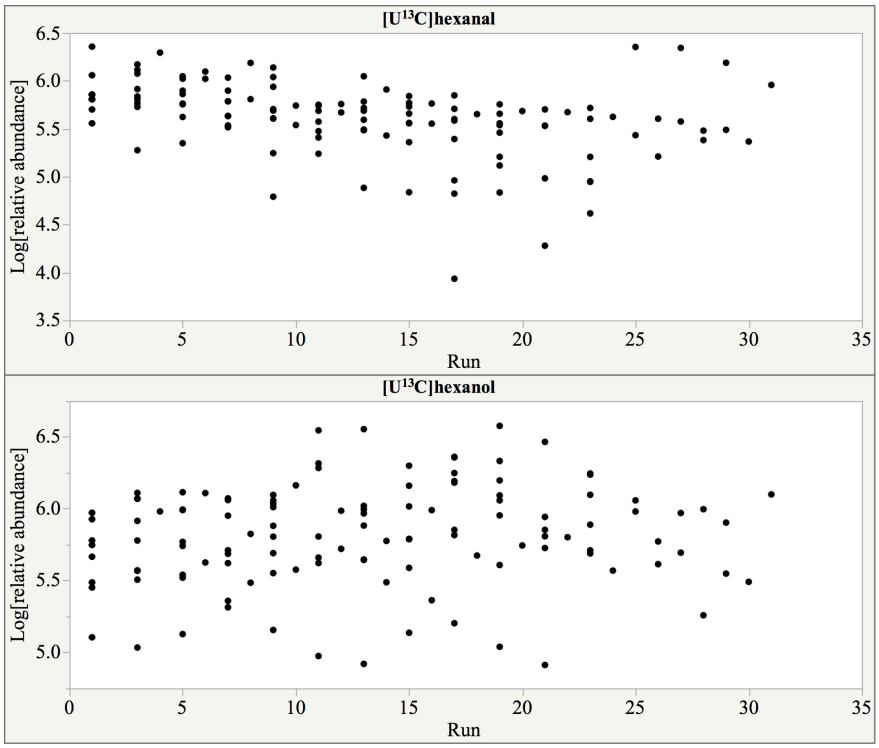

Figure S.2: Plot of ordinal run number (i.e. sample queue assignment) versus log-normalized peak areas for [U^{13}C]hexanal (top) and [U^{13}C]hexanol (bottom).

CHAPTER 3 SUPPLEMENTARY MATERIALS

Supplemental Table 1: Sample ID/Accession list and basic fruit chemistry

Section A. 2015 and 2016 samples

Year:	Collection Date:	Species:	Variety, if applicable:	Accession:	Avg. berry weight (g):	pH:	°Brix	Malate (g/L):	Malate (mg/berry):
2015	03 Aug.	Cinerea		171	0.29	3.07	3.3	11.3	3.2
2015	26 Aug.	Cinerea		171	0.39	3.00	5.5	25.6	9.8
2015	07 Oct.	Cinerea		171	0.50	2.92	9.2	23.8	11.5
2015	26 Aug.	Cinerea		588200	0.22	3.39	3.9	16.0	3.5
2015	07 Oct.	Cinerea		588200	0.35	2.78	12.2	30.3	10.2
2015	03 Aug.	Cinerea		588208	0.15	-	-	5.3	0.8
2015	26 Aug.	Cinerea		588208	0.24	2.83	4.0	18.0	4.3
2015	07 Oct.	Cinerea		588208	0.42	-	-	39.3	16.4
2015	03 Aug.	Cinerea		588218	0.12	2.81	4.0	3.9	0.5
2015	26 Aug.	Cinerea		588218	0.22	3.63	3.5	10.9	2.3
2015	07 Oct.	Cinerea		588218	0.31	2.80	8.4	36.2	11.0
2015	03 Aug.	Cinerea		588221	0.15	-	-	4.8	0.7
2015	26 Aug.	Cinerea		588221	0.29	2.75	4.1	18.3	5.2
2015	07 Oct.	Cinerea		588221	0.45	-	-	34.6	15.7
2015	26 Aug.	Cinerea		588398	0.17	2.98	3.1	11.2	1.9
2015	07 Oct.	Cinerea		588398	0.22	2.88	10.0	31.6	6.6
2015	03 Aug.	Cinerea		588460	0.12	3.10	3.6	5.6	0.6
2015	26 Aug.	Cinerea		588460	0.17	3.21	4.2	14.0	2.3
2015	07 Oct.	Cinerea		588460	0.24	2.94	13.3	29.7	6.7
2015	03 Aug.	Riparia		483165	0.56	2.73	5.6	24.9	13.6
2015	26 Aug.	Riparia		483165	0.65	3.19	11.5	19.4	12.1
2015	07 Oct.	Riparia		483165	0.73	3.31	16.5	13.4	9.2
2015	03 Aug.	Riparia		483172	0.38	2.69	4.6	22.1	8.2
2015	26 Aug.	Riparia		483172	0.55	2.91	10.1	22.7	11.9
2015	07 Oct.	Riparia		483172	0.47	3.13	22.6	17.8	7.7
2015	03 Aug.	Riparia		483173	0.60	3.03	3.7	17.3	10.2
2015	07 Oct.	Riparia		483173	0.75	3.02	15.5	10.4	7.4
2015	03 Aug.	Riparia		483174	0.51	2.61	4.7	15.7	7.8
2015	26 Aug.	Riparia		483174	0.68	2.83	11.5	27.0	17.6
2015	07 Oct.	Riparia		483174	0.75	3.06	17.1	19.4	13.6
2015	03 Aug.	Riparia		483176	1.43	2.79	3.8	19.6	27.6
2015	26 Aug.	Riparia		483176	2.00	-	-	15.4	30.7
2015	07 Oct.	Riparia		483176	1.76	3.32	16.9	6.8	11.2
2015	03 Aug.	Riparia		483181	1.67	2.50	6.5	26.0	42.2
2015	26 Aug.	Riparia		483181	2.00	2.93	12.3	17.3	33.1
2015	07 Oct.	Riparia		483181	2.00	3.34	11.5	9.4	17.9
2015	03 Aug.	Riparia		588167	0.49	3.01	4.2	17.9	8.7
2015	26 Aug.	Riparia		588167	0.65	3.06	14.7	20.1	12.4
2015	07 Oct.	Riparia		588167	0.77	3.56	13.3	14.1	10.3
2015	03 Aug.	Riparia		588261	0.34	2.77	5.7	21.9	7.4
2015	26 Aug.	Riparia		588261	0.50	3.25	18.5	18.8	8.7
2015	03 Aug.	Riparia		588304	0.49	2.94	3.8	11.3	5.5
2015	26 Aug.	Riparia		588304	0.22	3.25	7.9	21.3	4.5
2015	07 Oct.	Riparia		588304	0.21	3.02	11.6	15.8	3.2
2015	03 Aug.	Riparia		588346	0.21	2.74	6.9	21.7	4.4
2015	26 Aug.	Riparia		588346	0.46	2.91	16.8	15.7	6.8
2015	07 Oct.	Riparia		588346	0.43	2.89	14.4	11.4	4.7
2015	03 Aug.	Riparia		588347	0.45	-	4.5	20.8	9.3

2015	26 Aug.	Riparia		588347	0.59	2.92	17.7	19.3	10.6
2015	07 Oct.	Riparia		588347	0.64	3.21	21.7	16.4	9.7
2015	03 Aug.	Riparia		588436	0.52	2.80	4.8	18.9	9.6
2015	26 Aug.	Riparia		588436	1.00	3.90	14.2	7.9	7.5
2015	07 Oct.	Riparia		588436	0.97	3.86	14.7	5.6	5.2
2015	03 Aug.	Riparia		588438	0.18	2.72	4.6	27.9	4.9
2015	26 Aug.	Riparia		588438	0.58	3.11	12.7	23.0	12.6
2015	07 Oct.	Riparia		588438	0.53	3.32	18.4	15.8	7.8
2015	03 Aug.	Riparia		588440	0.17	2.90	3.2	9.0	1.5
2015	07 Oct.	Riparia		588440	0.25	3.07	20.2	15.6	3.6
2015	03 Aug.	Riparia		588483	0.34	2.63	6.3	32.4	10.8
2015	26 Aug.	Riparia		588483	0.51	3.04	15.7	31.9	15.3
2015	07 Oct.	Riparia		588483	0.53	3.11	20.3	19.0	9.3
2015	03 Aug.	Riparia		588562	0.42	2.52	6.6	26.7	10.9
2015	26 Aug.	Riparia		588562	0.64	3.05	20.1	21.5	12.7
2015	07 Oct.	Riparia		588562	0.71	3.09	23.8	9.5	6.2
2015	03 Aug.	Riparia		588565	0.61	2.76	6.5	28.6	17.1
2015	26 Aug.	Riparia		588565	0.71	3.01	13.4	26.3	17.8
2015	07 Oct.	Riparia		588565	0.65	3.03	19.1	22.4	13.6
2015	03 Aug.	Riparia		588711	0.45	2.68	5.5	26.2	11.6
2015	26 Aug.	Riparia		588711	0.54	2.89	14.2	30.2	15.3
2015	07 Oct.	Riparia		588711	0.52	2.81	18.3	20.7	10.0
2015	03 Aug.	Riparia		588586.b	0.53	2.75	4.7	17.4	9.0
2015	26 Aug.	Riparia		588586.b	0.67	3.05	12.0	23.1	14.7
2015	07 Oct.	Riparia		588586.b	0.67	3.27	14.5	17.0	10.7
2015	03 Aug.	Vinifera	Cabernet Franc	CF1	0.91	2.67	4.8	16.1	14.4
2015	26 Aug.	Vinifera	Cabernet Franc	CF1	1.43	3.08	14.2	7.1	9.6
2015	07 Oct.	Vinifera	Cabernet Franc	CF1	1.30	3.92	20.9	0.4	0.5
2015	03 Aug.	Vinifera	Cabernet Franc	CF2	0.94	2.81	3.5	12.9	12.0
2015	26 Aug.	Vinifera	Cabernet Franc	CF2	1.30	3.11	13.4	7.0	8.7
2015	07 Oct.	Vinifera	Cabernet Franc	CF2	1.36	3.87	21.6	1.7	2.2
2015	03 Aug.	Vinifera	Chardonnay	CH1	1.20	2.82	5.3	19.5	22.9
2015	26 Aug.	Vinifera	Chardonnay	CH1	1.58	3.13	14.1	8.9	13.3
2015	07 Oct.	Vinifera	Chardonnay	CH1	1.76	3.62	20.3	2.8	4.6
2015	03 Aug.	Vinifera	Chardonnay	CH2	0.94	2.71	4.2	15.8	14.5
2015	26 Aug.	Vinifera	Chardonnay	CH2	1.36	3.25	15.0	7.3	9.5
2015	07 Oct.	Vinifera	Chardonnay	CH2	1.76	3.74	21.5	3.4	5.5
2015	03 Aug.	Vinifera	Cabernet Sauvignon	CS1	0.91	2.88	4.5	17.4	15.6
2015	26 Aug.	Vinifera	Cabernet Sauvignon	CS1	1.30	3.11	13.8	8.6	10.6
2015	07 Oct.	Vinifera	Cabernet Sauvignon	CS1	1.50	3.68	22.2	2.3	3.2
2015	03 Aug.	Vinifera	Cabernet Sauvignon	CS2	0.73	2.85	4.4	17.3	12.4
2015	26 Aug.	Vinifera	Cabernet Sauvignon	CS2	1.25	3.24	15.5	8.1	9.5
2015	07 Oct.	Vinifera	Cabernet Sauvignon	CS2	1.58	3.67	21.1	2.5	3.6
2015	03 Aug.	Vinifera	Gewurztraminer	GW1	1.11	2.96	8.3	15.6	16.8
2015	26 Aug.	Vinifera	Gewurztraminer	GW1	1.58	3.58	17.2	3.5	5.1
2015	07 Oct.	Vinifera	Gewurztraminer	GW1	1.76	4.18	22.0	2.1	3.4
2015	03 Aug.	Vinifera	Gewurztraminer	GW2	0.71	2.97	4.5	21.6	15.1
2015	26 Aug.	Vinifera	Gewurztraminer	GW2	1.43	3.66	15.6	5.1	6.9
2015	07 Oct.	Vinifera	Gewurztraminer	GW2	1.58	4.05	20.9	2.8	4.1
2015	03 Aug.	Vinifera	Pinot Noir	PN1	0.88	2.81	6.7	22.2	19.1

2015	26 Aug.	Vinifera	Pinot Noir	PN1	1.07	3.41	14.1	6.0	6.1
2015	07 Oct.	Vinifera	Pinot Noir	PN1	1.07	3.57	20.8	2.8	2.8
2015	03 Aug.	Vinifera	Pinot Noir	PN2	0.75	2.76	5.9	22.2	16.3
2015	26 Aug.	Vinifera	Pinot Noir	PN2	1.30	3.44	15.5	6.0	7.4
2015	07 Oct.	Vinifera	Pinot Noir	PN2	1.50	3.73	21.0	1.8	2.5
2016	09 Aug.	Cinerea		171	0.23	2.85	6.3	14.6	3.3
2016	29 Aug.	Cinerea		171	0.31	2.66	7.2	23.9	7.2
2016	23 Sept.	Cinerea		171	0.38	2.57	15.3	24.9	9.0
2016	05 Oct.	Cinerea		171	0.48	2.83	16.8	24.1	10.9
2016	09 Aug.	Cinerea		588143	0.14	2.79	4.7	5.6	0.7
2016	29 Aug.	Cinerea		588143	0.23	2.60	5.7	27.6	6.1
2016	23 Sept.	Cinerea		588143	0.24	2.73	16.9	30.6	7.0
2016	05 Oct.	Cinerea		588143	0.28	2.75	19.9	31.3	8.2
2016	09 Aug.	Cinerea		588186	0.16	2.75	6.9	13.8	2.1
2016	29 Aug.	Cinerea		588186	0.20	2.57	5.3	19.0	3.8
2016	23 Sept.	Cinerea		588186	0.25	2.64	11.9	30.7	7.4
2016	05 Oct.	Cinerea		588186	0.33	2.77	16.6	27.5	8.6
2016	09 Aug.	Cinerea		588200	0.16	2.78	4.5	15.7	2.4
2016	29 Aug.	Cinerea		588200	0.19	2.74	5.0	24.8	4.7
2016	23 Sept.	Cinerea		588200	0.28	2.65	12.3	32.0	8.6
2016	05 Oct.	Cinerea		588200	0.28	2.90	16.9	35.7	9.2
2016	09 Aug.	Cinerea		588205	0.16	2.89	5.1	12.7	1.9
2016	29 Aug.	Cinerea		588205	0.20	2.89	5.8	22.0	4.3
2016	23 Sept.	Cinerea		588205	0.25	2.87	13.5	26.1	6.1
2016	05 Oct.	Cinerea		588205	0.35	3.16	16.8	22.4	7.4
2016	09 Aug.	Cinerea		588208	0.20	2.64	5.3	11.3	2.2
2016	29 Aug.	Cinerea		588208	0.32	2.74	5.0	22.8	7.2
2016	23 Sept.	Cinerea		588208	0.34	2.64	12.0	38.5	12.4
2016	05 Oct.	Cinerea		588208	0.42	2.64	16.9	34.3	13.4
2016	09 Aug.	Cinerea		588217	0.19	2.69	5.0	14.4	2.7
2016	29 Aug.	Cinerea		588217	0.29	2.55	5.4	29.7	8.5
2016	23 Sept.	Cinerea		588217	0.29	2.70	14.7	31.7	8.8
2016	05 Oct.	Cinerea		588217	0.35	2.69	17.5	31.2	10.3
2016	09 Aug.	Cinerea		588220	0.15	2.68	5.7	8.2	1.2
2016	29 Aug.	Cinerea		588220	0.19	2.54	5.1	26.2	5.0
2016	23 Sept.	Cinerea		588220	0.29	2.60	13.6	28.2	7.7
2016	05 Oct.	Cinerea		588220	0.38	2.69	17.7	27.7	10.0
2016	09 Aug.	Cinerea		588221	0.18	2.70	5.4	14.6	2.6
2016	29 Aug.	Cinerea		588221	0.21	2.62	4.5	19.5	4.1
2016	23 Sept.	Cinerea		588221	0.28	2.55	11.7	31.5	8.3
2016	05 Oct.	Cinerea		588221	0.35	2.57	15.6	30.8	10.2
2016	09 Aug.	Cinerea		588222	0.12	2.97	5.3	13.1	1.6
2016	29 Aug.	Cinerea		588222	0.21	2.89	5.1	24.3	5.0
2016	23 Sept.	Cinerea		588222	0.30	2.83	15.1	33.7	9.6
2016	09 Aug.	Cinerea		588398	0.13	2.75	4.7	12.6	1.7
2016	29 Aug.	Cinerea		588398	0.18	2.83	4.0	21.6	3.9
2016	23 Sept.	Cinerea		588398	0.23	2.61	10.8	38.7	8.4
2016	05 Oct.	Cinerea		588398	0.24	2.84	15.4	32.1	7.3
2016	09 Aug.	Cinerea		588460	0.16	2.85	4.6	9.0	1.4
2016	29 Aug.	Cinerea		588460	0.15	2.81	5.4	20.4	3.1

2016	23 Sept.	Cinerea		588460	0.21	2.76	11.3	32.0	6.4
2016	05 Oct.	Cinerea		588460	0.27	2.80	15.6	40.7	10.5
2016	09 Aug.	Cinerea		588575	0.19	2.64	5.4	9.7	1.8
2016	29 Aug.	Cinerea		588575	0.31	2.65	5.4	24.6	7.5
2016	23 Sept.	Cinerea		588575	0.32	2.69	10.8	31.6	9.6
2016	05 Oct.	Cinerea		588575	0.39	2.67	15.6	29.8	10.9
2016	09 Aug.	Cinerea		588678	0.12	2.84	5.1	7.4	0.8
2016	29 Aug.	Cinerea		588678	0.15	2.69	5.2	19.8	2.9
2016	23 Sept.	Cinerea		588678	0.22	2.77	13.8	26.7	5.5
2016	05 Oct.	Cinerea		588678	0.25	2.85	18.3	23.6	5.5
2016	09 Aug.	Cinerea		588685	0.20	3.18	3.4	5.5	1.1
2016	29 Aug.	Cinerea		588685	0.28	2.85	4.0	17.1	4.7
2016	23 Sept.	Cinerea		588685	0.30	2.88	8.4	26.1	7.7
2016	05 Oct.	Cinerea		588685	0.39	3.00	13.6	22.8	8.5
2016	04 Aug.	Hybrid	Chambourcin	CBe-1	0.64	2.62	6.4	18.8	11.7
2016	17 Aug.	Hybrid	Chambourcin	CBe-1	0.94	2.62	9.5	11.5	10.4
2016	29 Aug.	Hybrid	Chambourcin	CBe-1	1.30	2.98	15.1	5.3	6.5
2016	12 Sept.	Hybrid	Chambourcin	CBe-1	1.50	3.33	17.8	3.6	5.1
2016	23 Sept.	Hybrid	Chambourcin	CBe-1	1.58	3.40	19.4	3.1	4.5
2016	05 Oct.	Hybrid	Chambourcin	CBe-1	1.58	3.56	21.5	2.5	3.6
2016	04 Aug.	Hybrid	Corot Noir	CN-1	0.67	2.80	5.5	14.5	9.5
2016	17 Aug.	Hybrid	Corot Noir	CN-1	1.11	3.01	9.4	11.7	12.6
2016	29 Aug.	Hybrid	Corot Noir	CN-1	1.11	3.36	11.8	5.5	5.8
2016	12 Sept.	Hybrid	Corot Noir	CN-1	1.50	3.70	14.9	2.4	3.4
2016	23 Sept.	Hybrid	Corot Noir	CN-1	1.43	4.00	15.9	2.9	3.9
2016	05 Oct.	Hybrid	Corot Noir	CN-1	1.76	4.14	18.6	2.3	3.8
2016	04 Aug.	Hybrid	Vidal Blanc	VB-1	0.50	2.77	6.8	17.1	8.3
2016	17 Aug.	Hybrid	Vidal Blanc	VB-1	0.64	2.71	7.0	13.5	8.4
2016	29 Aug.	Hybrid	Vidal Blanc	VB-1	0.88	3.15	13.5	6.4	5.4
2016	12 Sept.	Hybrid	Vidal Blanc	VB-1	1.11	3.29	16.5	3.9	4.0
2016	05 Oct.	Hybrid	Vidal Blanc	VB-1	1.30	3.73	20.3	3.1	3.8
2016	04 Aug.	Hybrid	Vignoles	VL-1	0.49	2.69	8.2	17.4	8.3
2016	17 Aug.	Hybrid	Vignoles	VL-1	1.00	3.04	15.1	9.0	8.5
2016	29 Aug.	Hybrid	Vignoles	VL-1	1.00	3.34	20.8	6.2	5.7
2016	12 Sept.	Hybrid	Vignoles	VL-1	1.11	3.43	23.4	6.7	6.8
2016	09 Aug.	Riparia		255189	0.45	2.77	8.3	22.8	9.9
2016	29 Aug.	Riparia		255189	0.52	2.99	19.9	16.3	7.8
2016	23 Sept.	Riparia		255189	0.43	3.38	24.7	12.7	5.0
2016	09 Aug.	Riparia		483171	0.38	2.65	5.5	22.5	8.3
2016	29 Aug.	Riparia		483171	0.51	2.89	16.7	18.4	8.8
2016	23 Sept.	Riparia		483171	0.48	3.08	18.2	14.2	6.4
2016	05 Oct.	Riparia		483171	0.40	3.24	21.8	15.5	5.7
2016	09 Aug.	Riparia		483172	0.48	2.60	6.3	27.4	12.7
2016	29 Aug.	Riparia		483172	0.48	2.87	16.4	19.9	8.9
2016	23 Sept.	Riparia		483172	0.47	3.13	21.3	13.3	5.7
2016	09 Aug.	Riparia		483173	0.59	2.61	7.0	25.8	14.8
2016	29 Aug.	Riparia		483173	0.71	2.92	15.4	20.9	14.1
2016	23 Sept.	Riparia		483173	0.75	3.07	18.5	12.1	8.4
2016	05 Oct.	Riparia		483173	0.94	3.19	19.9	12.1	10.5
2016	09 Aug.	Riparia		483174	0.63	2.63	6.7	23.4	14.2

2016	29 Aug.	Riparia		483174	0.75	2.89	15.2	15.2	10.7
2016	23 Sept.	Riparia		483174	0.77	2.96	20.0	12.1	8.7
2016	05 Oct.	Riparia		483174	0.75	3.01	21.4	11.8	8.1
2016	09 Aug.	Riparia		588347	0.54	2.81	6.6	30.0	15.7
2016	29 Aug.	Riparia		588347	0.50	2.84	14.0	26.9	12.7
2016	23 Sept.	Riparia		588347	0.48	2.94	18.3	18.7	8.5
2016	05 Oct.	Riparia		588347	0.68	3.07	22.8	14.5	9.1
2016	09 Aug.	Riparia		588437	0.56	2.70	7.0	26.8	14.5
2016	29 Aug.	Riparia		588437	0.71	2.95	20.8	21.7	14.4
2016	23 Sept.	Riparia		588437	0.51	3.03	23.4	15.3	7.1
2016	05 Oct.	Riparia		588437	0.60	2.87	24.0	14.8	8.1
2016	09 Aug.	Riparia		588440	0.24	2.73	4.5	16.2	3.8
2016	29 Aug.	Riparia		588440	0.27	2.71	9.7	20.8	5.4
2016	23 Sept.	Riparia		588440	0.28	3.03	21.4	15.5	3.9
2016	09 Aug.	Riparia		588565	0.50	2.58	8.5	31.2	15.1
2016	29 Aug.	Riparia		588565	0.59	2.91	20.0	20.1	11.0
2016	23 Sept.	Riparia		588565	0.61	3.14	20.1	15.9	9.0
2016	09 Aug.	Riparia		588711	0.47	2.62	6.4	28.9	13.2
2016	29 Aug.	Riparia		588711	0.54	2.55	16.8	28.4	14.3
2016	23 Sept.	Riparia		588711	0.52	2.83	25.1	19.9	9.4
2016	04 Aug.	Vinifera	Cabernet Franc	CF-1	0.64	2.66	6.0	19.9	12.4
2016	17 Aug.	Vinifera	Cabernet Franc	CF-1	0.81	2.59	6.7	17.9	14.2
2016	29 Aug.	Vinifera	Cabernet Franc	CF-1	1.03	3.05	13.5	5.6	5.5
2016	12 Sept.	Vinifera	Cabernet Franc	CF-1	1.43	3.64	19.5	2.3	3.1
2016	23 Sept.	Vinifera	Cabernet Franc	CF-1	1.30	3.67	20.6	1.8	2.1
2016	05 Oct.	Vinifera	Cabernet Franc	CF-1	1.50	3.83	22.1	1.8	2.5
2016	04 Aug.	Vinifera	Lemberger	LB-1	0.54	2.64	6.2	15.1	7.9
2016	17 Aug.	Vinifera	Lemberger	LB-1	0.91	2.75	11.3	8.4	7.4
2016	29 Aug.	Vinifera	Lemberger	LB-1	1.36	3.21	13.3	2.8	3.7
2016	12 Sept.	Vinifera	Lemberger	LB-1	1.67	3.47	17.8	1.8	2.8
2016	23 Sept.	Vinifera	Lemberger	LB-1	1.36	3.70	20.7	2.0	2.5
2016	05 Oct.	Vinifera	Lemberger	LB-1	1.58	3.71	20.2	1.7	2.4
2016	04 Aug.	Vinifera	Riesling	RS90-1	0.65	2.72	5.2	20.2	12.9
2016	17 Aug.	Vinifera	Riesling	RS90-1	0.67	2.53	5.1	18.5	12.1
2016	29 Aug.	Vinifera	Riesling	RS90-1	1.00	3.02	13.4	8.2	7.8
2016	12 Sept.	Vinifera	Riesling	RS90-1	1.36	3.14	16.3	5.3	6.7
2016	23 Sept.	Vinifera	Riesling	RS90-1	1.15	3.31	19.2	3.0	3.2

Section B. Dissected berry pulp data									
Year:	Collection Date:	Species:	Variety, if applicable:	Accession:	Avg. berry weight (g):	pH:	Soluble sugars (g/100 g pulp):	Malate (g/Kg pulp):	Malate (mg/berry pulp):
2018	27 Sep.	Cinerea		588217	0.51	-	3.0	50.7	19.0
2018	31 Oct.	Cinerea		588217	0.46	-	11.1	47.9	15.9
2018	17 Sep.	Cinerea		588222	0.55	-	4.2	50.5	20.0
2018	19 Oct.	Cinerea		588222	0.55	-	10.8	47.8	19.4
2018	23 Aug.	Riparia		483171	0.48	-	6.1	30.6	10.4
2018	27 Sep.	Riparia		483171	0.64	-	10.5	22.9	11.7
2018	14 Aug.	Riparia		588483	0.58	-	7.8	44.2	18.4
2018	17 Sep.	Riparia		588483	0.70	-	13.9	27.0	14.0
2018	14 Aug.	Vinifera	Chardonnay		1.10	-	7.8	16.3	15.7
2018	17 Sep.	Vinifera	Chardonnay		1.55	-	18.2	2.3	3.3
2018	23 Aug.	Vinifera	Cabernet Franc		1.15	-	8.9	16.3	16.0
2018	27 Sep.	Vinifera	Cabernet Franc		1.52	-	20.1	1.9	2.5

Supplementary table 2. Proportion of skin, pulp, and seeds in berries of *Vitis* spp. Proportions were measured by the dissection of berries sampled during the 2018 growing season at two time-points: i) The onset of veraison (in parenthesis) and ii) 32 to 35 days post-veraison.

Specie	**Cultivar/accession**	**Skin (%w/w)**	**Seeds (%w/w)**	**Pulp (%w/w)**
Vinifera	Chardonnay	(6.11) 5.93	(6.39) 3.19	(87.5) 90.88
Vinifera	Cabernet Franc	(6.49) 7.65	(8.47) 5.6	(85.04) 86.75
Riparia	483171	(11.68) 6.23	(17.26) 14.25	(71.06) 79.52
Riparia	588483	(10.55) 10.64	(17.66) 15.7	(71.8) 73.66
Cinerea	588222	(11.4) 11.37	(16.34) 14.65	(72.26) 73.98
Cinerea	588217	(14.82) 16.14	(11.32) 12.14	(73.87) 71.73

Lab: Odorants as pH Indicators

FOR THE TEACHER

Submitted by
Gavin Sacks
Madeleine Bee
Elizabeth Chang
Cornell University
Ithaca, New York

Thanks to:
Sally B. Mitchell
Rye High School
Rye, New York

USDA-NSF EAGER Award
2017-67007-25940

Summary
In this lab, students will observe how the odor of common kitchen items (coffee, liquid aminos) change at different pH values, and relate this knowledge to their understanding of acid-base equilibrium.

Grade Level
High School

Objectives
By the end of this lab, students should be able to
- Define the term "odorant" and know the key chemical features necessary for a chemical to be an odorant
- Explain why the odor of some compounds change at as pH changes
- Define the term "pH indicator", and describe how both pigments and odorants can be used as pH indicators

Chemistry Topics
This lab supports students' understanding of
- Acids & Bases
- Indicators
- pH
- Chemoreception (human detection of chemical signals)

NGSS
This demonstration supports the following learning objectives:
- **NGSS Performance Expectation HS-PS3-6:** Students who demonstrate understanding can "refine the design of a chemical system by specifying a change in conditions that would produce increased amounts of products at equilibrium."
- The following NGSS are also met: Science & Engineering Practices (1), Disciplinary Core Ideas (2 and 3), and Crosscutting Concept (4):
  (1) **Constructing Explanations and Designing Solutions** -- explanations and designs that are supported by multiple and independent student-generated sources of evidence consistent with scientific ideas, principles, and theories.
  (2) **PS1-B Chemical Reactions** -- In many situations, a dynamic and condition-dependent balance between a reaction and the reverse reaction determines the numbers of all types of molecules present.
  (3) **ETS1.C Optimizing the Design Solution –** Criteria may need to be broken down into simpler ones that can be approached systematically, and decisions about the priority of certain criteria over others (trade-offs) may be needed.
  (4) **Stability and Change** -- Much of science deals with constructing explanations of how things change and how they remain stable.

AP Chemistry Curriculum Framework
This demonstration supports the following learning objectives:

- **Big Idea 6:** Any bond or intermolecular attraction that can be formed can be broken. These two processes are in a dynamic competition, sensitive to initial conditions and external perturbations.
    - **6.B:** Systems at equilibrium are responsive to external perturbations, with the response leading to a change in the composition of the system.
    - **6.C:** Chemical equilibrium plays an important role in acid-base chemistry and in solubility.

Time
Teacher Preparation: 15 minutes
Lesson: 60 minutes

Materials (per group)

- (5) 125 mL Erlenmeyer flasks with stoppers, or 200 mL jars with lids
- Citric acid, 14 g
- Pickling lime (CaOH), 7 g
- Instant coffee, ½ tsp dissolved in 50 mL hot water (per package instructions)
- Liquid aminos, 10 mL per group (soy sauce can be substituted, if needed)
- Acetic acid (white vinegar), 50 mL
- (4) pH strips
- Paper towels (for spills)

Safety

- Safety goggles and lab aprons must be work when handling chemicals in the lab.
- Do not drink any solutions! They are for smelling only.
- In the event of any of the solutions spilling on their skin, students should immediately rinse the area with water and inform the instructor.
- Clean-Up
    - Solutions can be dumped down the drain; flasks can be rinsed out.
    - Spills on the lab bench and/or on the floor should be cleaned up with paper towels.
    - Students should wash their hands thoroughly before leaving the lab.

Teacher Notes

- Students should have a basic understanding of pH, acid-base titrations, and equilibria
- Ideal group size is 2-3. The student roles are:
    - Sniffer: sniffs samples, evaluates intensity of aroma
    - Presenter: Selects a sample to present to sniffer
    - Data-Recorder (can be same as Presenter): Records data
- Differentiation (higher level):
    - Instead of, or in addition to, averaging group responses to volatile intensities, individual responses across the class could be plotted for a distribution analysis, and there could be a discussion on humans' differing sense of smell due to genetic variation
    - In keeping with AP Big Idea 6, students could explore changes in volatility due to other external perturbations to the system, e.g. salt additions and/or changes to system temperature

FOR THE STUDENT
Lesson

Aroma as a pH indicator

Background

Fresh baked bread? Hot chocolate? Dirty socks? Cat litter box? When you smell something, you are smelling chemicals. More specifically, you are smelling volatile (airborne) chemicals called *odorants*. These odorants trigger receptors at the top of your nasal cavity to generate the sensation of smell. Most real aromas, including baked bread and chocolate, result from the combined action of dozens of volatile chemicals. Put another way – no odorant compound smells just like "chocolate" all by itself.

However, a few common aromas are very simple. For example, "white vinegar" – the kind of vinegar commonly found in home kitchens – is a 5% solution of acetic acid (CH_3COOH) in water, the smell of vinegar is solely due to acetic acid[1].

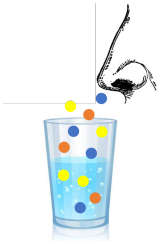

Most odorants in foods and beverages are not in the gas phase. For example, when a container (e.g. a test tube) is partially filled with vinegar, a small amout of acetic acid will volatize and enter the *headspace* – the space above the liquid. At room temperature, in a half-filled container, less than 1 out of 100000 acetic acid molecules will be in the headspace, with the rest still in the vinegar[2]. This ratio is typical of most odorants, and its useful to cooks – if the situation was reversed, we would only get one intense sniff of our food or drink, and then all of the aroma would be used up!

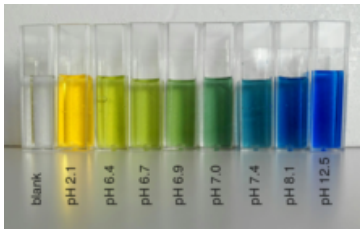

(Photo courtesy of Gregor Trefalt; Wikipedia.org)

Acetic acid can also be used as an "odorous" pH indicator. Typically, pH indicators are chemicals that change color when the pH of a solution changes. For example, bromothymol blue will appear yellow at a pH < 6 (acid), green between pH 6-8 (neutral), and blue at pH >8 (basic). The reason pH indicators change color is because they are weak acids and bases themselves, and their ability to absorb light changes as they gain or lose protons (H^+).

[1] Technically, acetic acid is not a simple odorant – it is also perceived by your sense of touch, causing an irritating sensation. For simplicity, we will treat both the odorous and tactile sensations caused by acetic acid as a smell.

[2] At low acetic acid concentrations, like vinegar, the relative proportion of acetic acid in the headspace and the liquid will be constant even if the acetic acid concentration is changed. This is described by Henry's Law, which is discussed in other lectures.

The situation is similar for acetic acid, except that instead of a color change, its volatility changes with pH. At low pH, acetic acid is protonated, and can be volatile. As pH increases, acetic acid loses a proton to form acetate (CH_3COO^-) which is non-volatile. This relationship is described by the Henderson-Hasselbach equation:

$$pH = pK_a + \log_{10}\left(\frac{[A^-]}{[HA]}\right)$$

Because the amount of acetic acid in the air above a solution is always proportional to the amount of acetic acid in solution, we expect to see the headspace concentration of acetic acid decrease as pH increases.

Likewise, the ratio of volatiles in the headspace and the protonation state of these odorants can change when a system is perturbed by the addition of a strong acid or base. In this case, we will be using liquid aminos and instant coffee with citric acid (acid) and pickling lime (base). Liquid aminos is very similar to soy sauce; liquid aminos are unfermented soy protein (while soy sauce is fermented) and liquid aminos contains less sodium than soy sauce. Both liquid aminos and soy sauce contain a host of amino acids and amino acid byproducts, like cadaverine and putrescine, which are chemical compounds associated with rotting cadavers and fishy smells. Similarly, when coffee beans are roasted, a range of volatile compounds are created, such as 2-furfurylthiol, which gives coffee a sulfury, roasty aroma, and 4-hydroxy-2,5-dimethyl-3(2H)-furanone, which has caramel-like notes.

Investigation Question
How will the odor of an acetic acid solution (white vinegar) change at low pH vs. high pH?

Hypothesis
Make a hypothesis statement below. Be sure to justify it with reasoning.

Pre-lab Questions

1. Based on the information above, sketch the distribution of acetic acid versus acetate in solution versus in the headspace at low pH.

2. How will the pickling lime be used for these experiements?

3. How do you expect the coffee to smell? List 5 descriptors.

Materials (per group)

- (5) 125 mL Erlenmeyer flasks with stoppers, or 200 mL jars with lids
- Citric acid, 14 g
- Pickling lime (CaOH), 7 g
- Instant coffee, ½ tsp dissolved in 50 mL hot water (per package instructions)
- Liquid aminos, 10 mL per group (soy sauce can be substituted, if needed)
- Acetic acid (white vinegar), 50 mL
- (4) pH strips
- Paper towels (for spills)

Safety

- Safety goggles and lab aprons must be work when handling chemicals in the lab.
- Do not drink any solutions! They are for smelling only.
- In the event of any of the solutions spilling on their skin, students should immediately rinse the area with water and inform the instructor.
- Clean-Up
    - Solutions can be dumped down the drain; flasks can be rinsed out.
    - Spills on the lab bench and/or on the floor should be cleaned up with paper towels.
    - Students should wash their hands thoroughly before leaving the lab.

Procedure

EXPERIMENT 1 – ODORANT INTENSITY IN SIMPLE SOLUTION VS. PH

Set Up – Experiment 1

1. Put on your safety equipment.
2. Obtain 5 clean flasks. Label the tubes as follows: water, low pH, medium-low pH, medium-high pH, high pH
3. Using a graduated cylinder, measure 10 mL of water, and pour it into the flask marked "water".
4. Weigh 4 g of citric acid and pour into the flask marked "low pH".
5. Weigh 2 g of citric acid and pour into the flask marked "medium-low pH".
6. Weigh 1 g of CaOH and pour into the flask marked "medium-high pH".
7. Weigh 2 g of CaOH and pour into the flask marked "high pH".
8. Using a graduated cylinder, add 10 mL of vinegar to each tube.
9. Stopper (cover) the flasks

Aroma Evaluation – Experiment 1

1. In each group, one person will be the "Sniffer", one person will be the "Presenter", and one person will be the "Recorder". The Presenter will sit with the flasks several feet away from the Recorder and Sniffer.
2. The Sniffer will hold the water+vinegar flask. The presenter will keep the other pH adulterated flasks.
3. The Presenter will select one of the pH solution flasks at random, show the label to the Recorder, and then give the flask to the Sniffer. The Sniffer should <u>not</u> look at the label.
4. The Sniffer should swirl the flask, removed the stopper, sniff the solution by wafting the aroma toward their nose, then tells the Recorder how strong the vinegar aroma is on a scale of 0 (no aroma) to 10 (as strong as the vinegar+water tube).
5. The Recorder notes the sniffer's rating.
6. The Sniffer then hands the pH adulterated flask back to the Presenter.
7. The Presenter repeats steps 3-5 with a different pH flask each time until four flasks have been sniffed and evaluated
8. The Presenter, Sniffer, and Recorder then change roles, until all group members have sniffed the samples and evaluated the vinegar aroma

Data - Experiment 1

Data Table 1: Vinegar aroma vs. pH					
		Vinegar intensity, 0-10 scale: Reference: No vinegar odor = 0, vinegar+water tube odor = 10			
Solution		Sniffer 1 (name)	Sniffer 2 (name)	Sniffer 3 (name)	Average
Low pH					
Med. - low pH					
Med. – high pH					
High pH					

EXPERIMENT 2 – ODORANT PERCEPTION IN COMPLEX MIXTURES VS. PH

Set Up – Experiment 2

1. Keep your safety equipment on
2. Rinse out your flasks with clean water until they no longer smell like vinegar.
3. Label the four flasks as A (aminos at low pH), B (aminos at high pH), C (coffee at low pH), and D (coffee at high pH).
4. Using a graduated cylinder, add the following
    a. 45 mL water to flasks A and B,
    b. 5 mL liquid aminos to flasks A and B
    c. 50 mL instant coffee (1/2 tsp in 50 mL hot water – per package instructions) to flasks C and D.
5. Weigh (2) 4 g quantities of citric acid
6. Weigh (2) 2 g quantities of CaOH
7. Add 4 g of citric acid to flask A; add 4 g of citric acid to flask C
8. Add 2 g of CaOH to flask B; add 2 g of CaOH to flask D
9. Stopper all flasks
10. Swirl, remove stopper, hold flask 1-2” from nose, and waft aromas toward nose
11. Using a glass pipet or other instrument to transfer 1 drop of each solution to a pH strip to determine final pH for each jar.

Liquid aminos and instant coffee at low and high pH.

Aroma Evaluation – Experiment 2

Data Table 1: Odor character vs. pH for liquid aminos and instant coffee					
		Odor description (1-3 words per sniffer)			
Solution	Sample	Sniffer 1 (name):	Sniffer 2 (name):	Sniffer 3 (name):	
Low pH	Instant coffee				
High pH	Instant coffee				
Low pH	Liquid aminos				
High pH	Liquid aminos				

1. Each group member sniffs each solution, and records what they think it smells like (1-3 word descriptions)

Data - Experiment 2

Analysis - Experiment 1

1. Create a bar graph that compares Vinegar Aroma (average) vs. pH

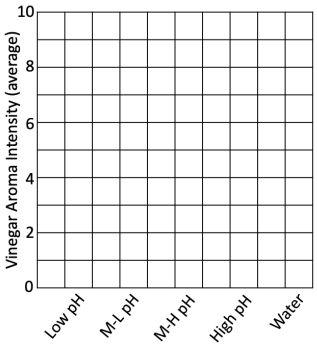

2. Explain your graph.

Analysis - Experiment 2

1. How did the aroma of the low pH instant coffee compare to the high pH instant coffee?

2. How did the aroma of the low pH liquid aminos compare to high pH liquid aminos?

Conclusions

1. β-damascenone is an odorant associated with rose or floral aromas. It is found in many food stuffs, including coffee and apple cider vinegar.
    a. Draw it's expected molecular charge at both low and high pH.
    b. How do you expect a change in the pH to affect the aroma?

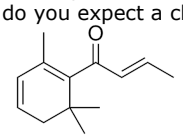

2. 3-methylbutanoic acid is one of the key odorants (by OAV, or odor-activity value) in soy sauce. It contributes a sweaty, cheesy aroma.
    a. Draw it's expected molecular charge at both low and high pH.
    b. How do you expect a change in the pH to affect the aroma?

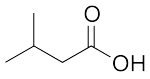

3. Putrescine and cadaverine are amino acid derived aromas that are released from the amino acids via decarboxylation at the **α**-carbon. Use retrosynthetic analysis to determine their amino acid precursors. Draw the amino acid below, and show where cleavage occurs.

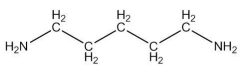

Cadaverine

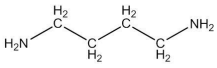

Putrescine

4. You are a flavor scientist at a major food company (yes, this is a real career path!). They want to combine two trendy topics: cold brew coffee and alkaline water, to create an alkaline cold brew coffee (pH of 9). Based on your knowledge of aroma chemistry, explain why you think this idea is advisable or inadvisable.

Student Assessment

Student Knowledge, Attitudes, and Behaviors Assessment

Directions:
Read each of the following statements or questions below and choose the BEST answer from the choices given.

1) At high pH, an acid is _____. When the pH is lowered, the acid will _____ a proton.
   a) deprotonated; lose
   b) deprotonated; gain
   c) protonated; lose
   d) protonated; gain

2) Describe the flavor of your favorite food:

3) The volatility of odorants in a solution (ratio of volatiles in the solution versus in the headspace) can be changed by:
   a) Adding salt to the solution
   b) Putting the solution in an ice bath
   c) Dividing the solution into 2 vials
   d) A and B only
   e) A, B and C

4) Odorants are made up of volatile chemicals:
   a) Yes
   b) No
   c) Maybe
   d) Unsure

5) When you hear the word “matrix”, what comes to mind? Circle all that apply.
   a) A rectangular array of numbers, symbols, or expressions
   b) A sci-fi movie starring Keanu Reeves
   c) A compact car made by Toyota
   d) Differences in pH, temperature, and macromolecules in a food or beverage that can change the volatility of odorants

6) Taste is the same thing as flavor.
   a) True
   b) False

7) The five types of taste receptors are salty, sour, sweet, bitter, and umami.
   a) True
   b) False

8) The pH of a food or beverage affects how it smells to us.
   a) True
   b) False

9) Referencing your response to question 2, circle what senses you mentioned when describing your favorite food:
   a) How it looks (before eating it)
   b) How it smells before I bite into it
   c) How it tastes
   d) How it smells while I'm chewing it
   e) How it feels in my mouth

10) Are you familiar with the term "food science"?
   a) Yes
   b) No
   c) Maybe
   d) Unsure

11) Are you familiar with the term "flavor chemistry"?
   a) Yes
   b) No
   c) Maybe
   d) Unsure

12) Would you like to learn more about careers in food science and/or flavor chemistry?
   a) Yes
   b) No
   c) Maybe
   d) Unsure